International Journal of Biological Macromolecules 239 (2023) 124232

Contents lists available at ScienceDirect

International Journal of Biological Macromolecules

journal homepage: www.elsevier.com/locate/ijbiomac

Discovery of novel benzenesulfonamides incorporating 1,2,3-triazole scaffold as carbonic anhydrase I, II, IX, and XII inhibitors

Aida Buza [a,b], Cüneyt Türkeş [c,*], Mustafa Arslan [b,*], Yeliz Demir [d], Busra Dincer [e], Arleta Rifati Nixha [a], Şükrü Beydemir [f,g]

[a] Department of Chemistry, Faculty of Mathematical and Natural Sciences, Pristina University, 10000, Republic of Kosova, Albania
[b] Department of Chemistry, Faculty of Arts and Science, Sakarya University, 54187, Sakarya, Turkey
[c] Department of Biochemistry, Faculty of Pharmacy, Erzincan Binali Yıldırım University, 24002 Erzincan, Turkey
[d] Department of Pharmacy Services, Nihat Delibalta Göle Vocational High School, Ardahan University, 75700 Ardahan, Turkey
[e] Department of Pharmacology, Faculty of Pharmacy, Erzincan Binali Yıldırım University, 24002 Erzincan, Turkey
[f] Department of Biochemistry, Faculty of Pharmacy, Anadolu University, 26470 Eskişehir, Turkey
[g] Bilecik Şeyh Edebali University, 11230 Bilecik, Turkey

ARTICLE INFO

Keywords:
Carbonic anhydrase
Benzenesulfonamide
Selective inhibitor
Cytotoxicity
In silico study

ABSTRACT

Sulfonamides are among the most promising potential inhibitors for carbonic anhydrases (CAs), which are pharmaceutically relevant targets for treating several disease conditions. Herein, a series of benzenesulfonamides bearing 1,2,3-triazole moiety as inhibitors of human (*h*) α-CAs (*h*CAs) were designed using the tail approach. The design method combines a benzenesulfonamide moiety with a tail of oxime and a zinc-binding group on a 1,2,3-triazole scaffold. Among the synthesized derivatives, the naphthyl (**6m**, K_I of 68.6 nM, S_I of 10.3), and methyl (**6a**, K_I of 56.3 nM, S_I of 11.7) derivatives (over *h*CA IX) and propyl (**6c**, K_I of 95.6 nM, S_I of 2.7), and pentyl (**6d**, K_I of 51.1 nM, S_I of 6.6) derivatives (over *h*CA XII) displayed a noticeable selectivity for isoforms *h*CA I and II, respectively. Meanwhile, derivative **6e** displayed a potent inhibitory effect versus the cytosolic isoform *h*CA I (K_I of 47.8 nM) and tumor-associated isoforms *h*CA IX and XII (K_Is of 195.9 and 116.9 nM, respectively) compared with the reference drug acetazolamide (AAZ, K_Is of 451.8, 437.2, and 338.9 nM, respectively). Derivative **6b** showed higher potency (K_I of 33.2 nM) than AAZ (K_I of 327.3 nM) towards another cytosolic isoform *h*CA II. Nevertheless, substituting the lipophilic large naphthyl tail to the 1,2,3-triazole linked benzenesulfonamides (**6a-n**) raised inhibitory effect versus *h*CA I and XII and selectivity towards *h*CA I and II isoforms over *h*CA IX. Evaluation of the cytotoxic potential of the synthesized derivatives was conducted in L929, MCF-7, and Hep-3B cell lines. Several compounds in the series demonstrated significant antiproliferative activity and minimal cytotoxicity. In the molecular docking study, the sulfonamide moiety interacted with the zinc-ion and neatly fit into the *h*CAs active sites. The extension of the tail was found to participate in diverse hydrophilic and hydrophobic interactions with adjacent amino acids, ultimately influencing the effectiveness and specificity of the derivatives.

1. Introduction

Sulfonamides constitute a significant class of sulfa drugs [1] and have become significant species of pharmacophores thanks to their unique properties such as less toxicity, oral absorption, cost-effectiveness, and increased reactivity [2]. Due to the numerous biological activities, including antibacterial [3], anti-inflammatory [4], anti-viral [5], and anti-diabetic activity [6], thousands of sulfonamide derivatives were synthesized and widely used to treat various diseases [7]. Furthermore, in recent years, triazole compounds have gained special attention based on their solid pharmacological activity, low toxicity [8], high bioavailability and stability [9], suitable pharmacokinetics property [10], broad spectrum [11], and better curative effect [12,13]. Oxime ethers have important motifs due to their significant medicinal chemistry applications and presence in many medicinal and various pharmaceutical products [14]. They have become increasingly popular in pharmaceutical synthesis due to their biological properties, such as antifungal [15], antibacterial [16], anti-inflammatory [17],

* Corresponding authors.
E-mail addresses: cuneyt.turkes@erzincan.edu.tr (C. Türkeş), marslan@sakarya.edu.tr (M. Arslan).

https://doi.org/10.1016/j.ijbiomac.2023.124232
Received 4 January 2023; Received in revised form 17 March 2023; Accepted 25 March 2023
Available online 30 March 2023

anticonvulsant [18], and antitumor [19] (Fig. 1).

Both prokaryotes and eukaryotes have the ubiquitous class of zinc-containing metalloenzymes known as carbonic anhydrase (EC 4.2.1.1, CA) [20–23]. These metalloenzymes effectively catalyze carbon dioxide's reversible essential hydration. [24,25]. Because the bicarbonate and proton ions formed as a result of this reaction are some cornerstones in maintaining the acid-base balance in most living things [26–28]. In addition to maintaining pH balance, they are essential for biosynthetic reactions, carbon dioxide, bicarbonate transport, electrolyte secretion, bone resorption, calcification, and many other physiological functions [29,30]. Humans only have one subset of the α-class, known as human-associated carbonic anhydrases (*h*CAs), which are further divided into fifteen isoforms based on their catalytic activity, tissue distribution, subcellular localization, and inhibitor affinities [31–33]. Some of these fifteen *h*CAs are catalytically active: (i) Cytosolic isoforms, *h*CA I, II, III, VII, and XIII; (ii) Membrane-bound isoforms, *h*CA IV, IX, XII, and XIV; (iii) Mitochondrial isoforms, *h*CA VA and VB; and (iv) A secreted *h*CA VI isoform [34–36]. It is undeniable that these *h*CAs contribute significantly to many physiological processes through their regular expression and tightly controlled activity. However, their involvement in numerous pathological processes is also well known due to their overexpression and uncontrolled activity, which contribute to several diseases [37–39]. For instance, cerebral/retinal edema is linked to overexpression of the *h*CA I isoform; the *h*CA II is connected to altitude sickness, edema, epilepsy, and glaucoma. Whereas overexpression of the *h*CA IX is linked to cancer, the *h*CA IV isoform is associated with glaucoma, pigmentosa, retinitis, and stroke [40]. The roles of these *h*CAs in the various pathological conditions mentioned above clearly demonstrate their importance as potential therapeutic drug targets. Additionally, because the active site architecture of all twelve catalytically active *h*CAs is similar [41,42], it is important to create selective inhibitors of a particular isoform in order to generate good leads that can be further developed into medicines without the disparate side effects frequently associated with off-target inhibition. Despite discovering other techniques for producing selective *h*CA inhibitors (*h*CAIs), the "tail approach" proved to be the most effective and popular [43,44]. In fact, it has been claimed that practically all drug design studies conducted during the past ten years have considered this strategy [45]. The process involves introducing multiple chemical appendages, such as primary sulfamoyl and carboxylic acid functional groups, onto an aromatic or heterocyclic ring bearing a zinc-binding moiety through a flexible linker.

As an extension of our research aimed at developing highly efficacious and specific inhibitors of *h*CAs, the present investigation is focused on evaluating the impact of the tail approach on the inhibitory activity and selectivity of the synthesized compounds towards different *h*CA isoforms [46]. Different spectroscopic techniques were employed to ascertain the structural features of the novel synthesized 1,2,3-triazole benzenesulfonamide substituted oxime ether derivatives (**6a-n**) in this approach (Scheme 1). Subsequently, the inhibitory effects of the synthesized derivatives were assessed on four human carbonic anhydrase isoforms, namely *h*CA I, II, IX, and XII. Additionally, molecular docking analyses were carried out to elucidate the theoretical binding mechanisms of the novel compounds (**6a-n**) with the active sites of the target *h*CAs.

2. Results and discussions

2.1. Drug design strategy and chemistry

Given the marked similarity among the active sites of various *h*CA isoforms, the tail technique has emerged as one of the most promising strategies for the design and synthesis of *h*CAIs [47]. This strategy involves appending diverse aryl or heterocyclic frameworks to the aromatic sulfonamide ring of *h*CAIs to selectively target hydrophobic or hydrophilic residues in the outer region of the isoform's active site [48]. The target compounds (**6a-n**) possess a benzenesulfonamide zinc-binding group attached to a rigid triazole scaffold, ensuring that the compound's tail is properly oriented towards the hydrophobic or hydrophilic rims of the active site. By establishing favorable interactions with specific residues in the hydrophilic region of the active site, the 1,2,3-triazole moiety increases the flexibility and hydrophilicity of the designed compounds, thereby imparting selectivity towards *h*CA IX. For

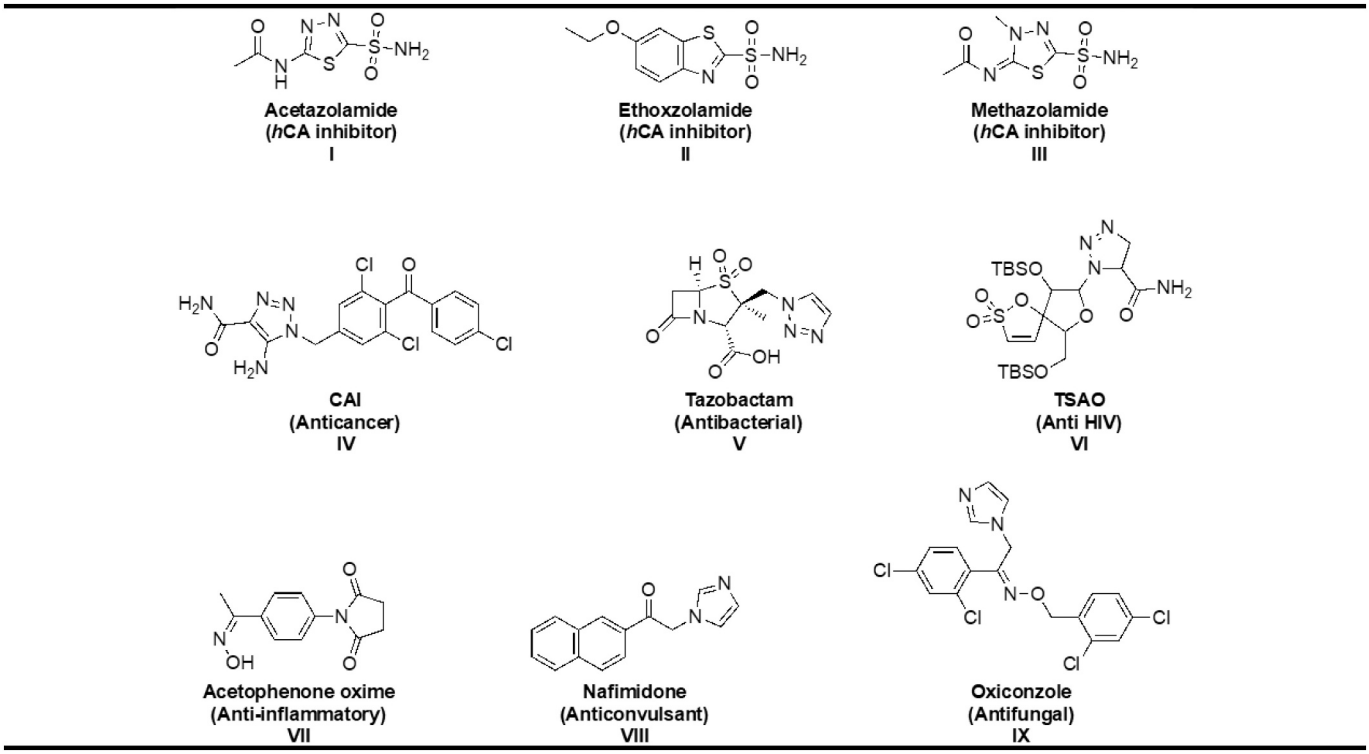

Fig. 1. Some clinically used sulfonamide (I-III), 1,2,3-triazole (IV-VI), and oxime ether (VII-IX) based drugs.

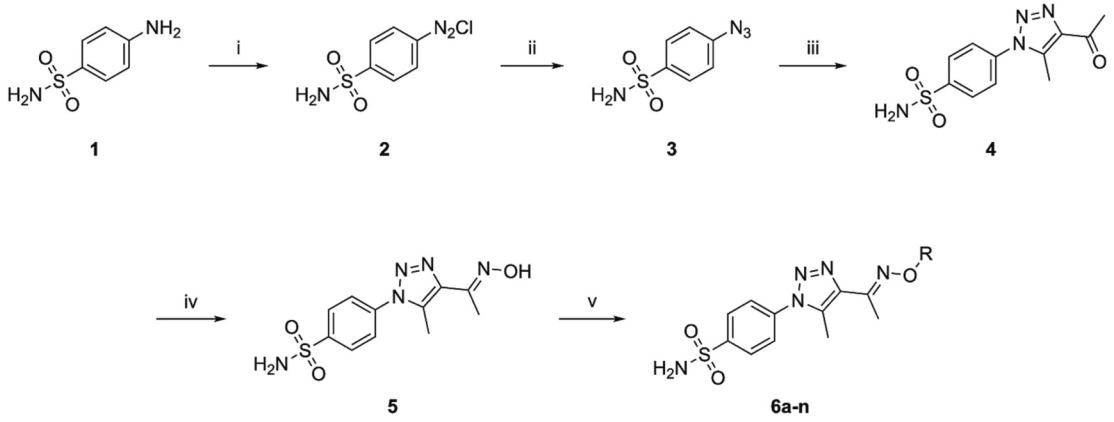

Compound ID	R	Compound ID	R	Compound ID	R
6a	Methyl	**6f**	Nonyl	**6k**	Diethylacetylamide
6b	Ethyl	**6g**	Allyl	**6l**	Benzyl
6c	Propyl	**6h**	n-Butenyl	**6m**	Naphthyl
6d	Pentyl	**6i**	Propargyl	**6n**	Anthryl
6e	Heptyl	**6j**	Acetylamide		

Scheme 1. Synthetic pathway of target 1,2,3-triazole benzenesulfonamide substituted oxime ethers (**6a-n**). (i) H_2O/HCl, $NaNO_2$; (ii) NaN_3; (iii) Acetyl acetone, DMSO, K_2CO_3; (iv) DMF/Et_3N, NH_2OH/HCl; (v) R-X/NaOH/TBAB, DMSO.

this reason, the different elongated linkers were employed to manipulate the *h*CA inhibitory effect of the target compounds (**6a-n**). The hydrophobic tail was also synthesized using the 1,3-dioxoisoindoline-5-carboxylate moiety.

In this study, 14 novel oxime ether-linked 1,4-disubstituted 1,2,3-triazole sulfonamides (**6a-n**) have been synthesized starting from benzenesulfonamide by 1,3 dipolar cycloadditions of 4-(4-hydroxyimino) ethyl)-5-methyl -2*H*-1,2,3-triazol-2yl)benzenesulfonamide (**5**) and alkyl or aryl halides (Scheme 1). The synthesized compounds were characterized using FT-IR, ^{1}H NMR, ^{13}C NMR, and mass spectrometry and their spectra of the compounds (**6a-n**) were given in Supplementary Material.

From the ^{1}H NMR spectra, sulfanilamide NH_2 and the = CH proton peaks on aromatic ring resonances at around 7.60 ppm and between 7.00 and 8.00 ppm, respectively. CH_3 protons are seen around 2.4 and 2.6 ppm, and Methyl or methylene attached to oxime-ether comes around 4.2 ppm. In the ^{13}C NMR spectra, Carbon atom attached to oxygen atom resonance at around 70 ppm and carbon atom bonded to NOR with double bond comes around 150 ppm. Carbon atoms in triazole ring are seen at around 130 and 140 ppm.

In the infrared spectra of compounds **6a-n**, it was possible to observe the absorptions between 3200 and 3350 cm^{-1} relating to NH_2 peaks. As seen in the literature [49], two peaks are assigned to SO_2 as symmetric and asymmetric stretching. The asymmetric and symmetric stretch peaks were appeared around 1350 and 1160 cm^{-1}, respectively. Aliphatic C—H and C═C bond absorption peaks were seen around 2990 and 1550 cm^{-1}, respectively. C═NO double bond peaks were appeared around 1590 cm^{-1}. In the compound 6i, the hydrogen bonded to triple bond comes around 3300 cm^{-1}. All spectra support the structure of the synthesized compounds.

2.2. Carbonic anhydrase inhibitory effect of the target compounds

The inhibitory potential of the 1,2,3-triazole benzenesulfonamide substituted oxime ether derivatives (**6a-n**) was evaluated against four physiologically and pharmacologically relevant *h*CA isoforms cytosolic *h*CA I and II, as well as transmembrane *h*CA IX and XII, using the esterase assay according to Verpoorte's method. Acetazolamide (AAZ, PubChem CID: 1986), a commonly prescribed medication, was utilized as a reference inhibitor in the assays, despite its lack of specificity towards a particular *h*CA isoform. Table 1 summarizes the inhibition constants (K_I) and their corresponding coefficient of determination (R^2) for the tested enzymes.

The cytosolic isoform *h*CA I was potently inhibited by 1,2,3-triazole benzenesulfonamide substituted oxime ethers (**6a-n**) with K_Is in the low nanomolar range of 47.8–257.6 nM, indicating that all synthesized compounds (**6a-n**) are more potent inhibitors than reference drug AAZ (K_I of 451.8 nM). The most active derivatives in this series enclose heptyl **6e**, naphthyl **6m**, and ethyl **6b** groups, which have K_Is of 47.8, 68.6, and 75.9 nM, respectively. Compounds having acetylamide **6j** and propargyl **6i** groups exhibited K_Is of 195.0 and 197.5 nM, respectively, whilst the weakest inhibitor in this group, **6l**, which has a K_I of 257.6 nM, incorporates the benzyl group.

The inhibitory potential of the 1,2,3-triazole benzenesulfonamide substituted oxime ether derivatives (**6a-n**) reported herein was investigated, and all compounds exhibited potent inhibition against the physiologically prominent *h*CA II isoform, with K_Is ranging from 33.2 to 248.3 nM. This potency was even superior to that of the conventional drug AAZ, which exhibited a K_I of 327.3 nM. Notably, the ethyl derivative **6b** displayed the most effective inhibition of *h*CA II, with a K_I in the two-digit nanomolar range (33.2 nM). Derivatives **6c** and **6f** also demonstrated potent inhibition of *h*CA II, with K_Is in the two-digit nanomolar range (40.4 and 42.2 nM, respectively), while compounds

Table 1
Inhibition data of human CA isoforms *h*CA I, II, IX, and XII with novel synthesized 1,2,3-triazole benzenesulfonamide substituted oxime ethers (**6a-n**) and the reference inhibitor acetazolamide, a clinically used drug.

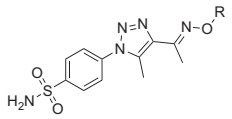

6a-n

Compounds		*h*CA I		*h*CA II		*h*CA IX		*h*CA XII	
ID	R	K_I [a] (nM)	R^2	K_I [a] (nM)	R^2	K_I [a] (nM)	R^2	K_I [a] (nM)	R^2
6a	Methyl	124.9 ± 24.1	0.9478	56.3 ± 12.5	0.9315	660.0 ± 73.2	0.9634	284.3 ± 36.0	0.9771
6b	Ethyl	75.9 ± 11.6	0.9659	33.2 ± 6.7	0.9480	228.0 ± 31.2	0.9782	192.3 ± 28.5	0.9711
6c	Propyl	95.6 ± 16.7	0.9591	40.4 ± 8.8	0.9349	394.4 ± 43.5	0.9633	258.9 ± 53.8	0.9447
6d	Pentyl	171.9 ± 28.9	0.9647	51.2 ± 12.0	0.9328	298.3 ± 46.3	0.9689	337.3 ± 63.8	0.9546
6e	Heptyl	47.8 ± 8.5	0.9519	64.7 ± 14.5	0.9391	195.9 ± 26.4	0.9710	116.9 ± 18.3	0.9650
6f	Nonyl	95.8 ± 14.2	0.9718	42.2 ± 7.4	0.9558	200.7 ± 28.2	0.9745	147.8 ± 26.0	0.9626
6g	Allyl	108.3 ± 19.7	0.9495	61.0 ± 10.8	0.9516	241.9 ± 34.5	0.9682	231.3 ± 41.9	0.9533
6h	n-Butenyl	121.3 ± 20.5	0.9595	83.3 ± 13.6	0.9624	456.3 ± 65.4	0.9734	216.7 ± 32.5	0.9661
6i	Propargyl	197.5 ± 26.8	0.9735	159.1 ± 26.4	0.9643	443.0 ± 81.2	0.9589	403.5 ± 78.2	0.9494
6j	Acetylamide	195.0 ± 31.0	0.9656	159.0 ± 25.8	0.9713	1072 ± 111	0.9810	207.6 ± 43.3	0.9379
6k	Diethylacetylamide	81.6 ± 11.1	0.9731	74.7 ± 13.0	0.9631	254.4 ± 46.5	0.9624	151.5 ± 30.9	0.9390
6l	Benzyl	257.6 ± 48.2	0.9491	248.3 ± 33.9	0.9770	528.0 ± 93.4	0.9590	558.6 ± 110.5	0.9606
6m	Naphthyl	68.6 ± 8.9	0.9750	63.3 ± 14.4	0.9346	704.8 ± 86.5	0.9742	120.8 ± 19.1	0.9657
6n	Anthryl	167.0 ± 26.9	0.9622	176.6 ± 32.3	0.9619	297.9 ± 45.0	0.9718	254.2 ± 58.0	0.9336
AAZ [b]	–	451.8 ± 59.1	0.9398	327.3 ± 32.8	0.9712	437.2 ± 53.9	0.9420	338.9 ± 33.4	0.9688

[a] The test results were expressed as means of triplicate assays ± SEM.
[b] Acetazolamide.

6i, **6n**, and **6l** exhibited weaker inhibitory activity, with K_Is in the three-digit nanomolar range (159.1, 176.6, and 248.3 nM, respectively).

All of the newly synthesized 1,2,3-triazole benzenesulfonamide substituted oxime ether derivatives (**6a-n**) were found to exhibit inhibitory activity towards the transmembrane tumor-associated *h*CA IX isoform, with K_Is ranging from three to four digits (195.9–1072 nM). Notably, the heptyl **6e**, nonyl **6f**, ethyl **6b**, allyl **6g**, and diethylacetylamide **6k** derivatives displayed potent inhibition, with K_Is of 195.9, 200.7, 228.0, 241.9, and 254.4 nM, respectively, surpassing that of the standard drug AAZ (K_I of 437.2 nM). Furthermore, the anthryl **6n** derivative (K_I of 297.9 nM) demonstrated activity equivalent to that of the pentyl **6d** derivative (K_I of 298.3 nM). Conversely, the methyl **6a**, naphthyl **6m**, and acetylamide **6j** derivatives exhibited the weakest inhibition within the group, with K_Is of 660.0, 704.8, and 1072 nM, respectively.

The 1,2,3-triazole benzenesulfonamide substituted oxime ether compounds **6a-n** were found to effectively inhibit the transmembrane tumor-associated *h*CA XII isoform with K_I values ranging from 116.9 to 558.6 nM, which is superior to the reference drug AAZ (K_I of 338.9 nM). Notably, heptyl **6e**, naphthyl **6m**, nonyl **6f**, diethylacetylamide **6 k**, and ethyl **6b** derivatives displayed robust inhibition of *h*CA XII with K_I values <200 nM, while the benzyl **6l** derivative exhibited the weakest inhibition (K_I of 558.6 nM).

Table 2
Selectivity indexes for the inhibition of cytosolic *h*CA I and II isoforms over transmembrane *h*CA IX and XII isoforms for targeted 1,2,3-triazole benzenesulfonamide substituted oxime ethers (**6a-n**).

Compounds ID	Selectivity index[a]			
	IX/I	IX/II	XII/I	XII/II
6a	5.3	11.7	2.3	5.0
6b	3.0	6.9	2.5	5.8
6c	4.1	9.8	2.7	6.4
6d	1.7	5.8	2.0	6.6
6e	4.1	3.0	2.4	1.8
6f	2.1	4.8	1.5	3.5
6g	2.2	4.0	2.1	3.8
6h	3.8	5.5	1.8	2.6
6i	2.2	2.8	2.0	2.5
6j	5.5	6.7	1.1	1.3
6k	3.1	3.4	1.9	2.0
6l	2.0	2.1	2.2	2.2
6m	10.3	11.1	1.8	1.9
6n	1.8	1.7	1.5	1.4

[a] Selectivity index (S_I) of inhibitors for *h*CA I and II over off-targets isoforms, *h*CA IX and XII, calculated as the ratio of K_I off-target *h*CA/K_I target *h*CA. A high-value ratio characterizes a potent, selective inhibitor.

2.3. SARs parameters of the target compounds

The findings presented in Tables 1 and 2 provided insights into the structure-activity relationships (SARs) of the compounds investigated. Regarding SAR, replacing the benzyl (**6l**, K_I of 257.6 nM) or anthryl rings (**6n**, K_I of 167.0 nM) with a linear alkyl chain raised the inhibitory effect against the cytosolic isoform *h*CA I by 9.5 and 6.0 times compared to AAZ, as seen in the heptyl **6e** and ethyl **6b** derivatives (K_Is of 47.8 and 75.9 nM, respectively). Also, as with **6m**, replacing the benzyl ring with the more lipophilic naphthalene group significantly increased the inhibitory effect versus *h*CA I.

The reduction of the inhibition potent against *h*CA II was observed when the linear alkyl chains were elongated as in ethyl **6b**, propyl **6c**, pentyl **6d**, and heptyl **6e** derivatives (K_Is of 33.2, 40.4, 51.1, and 64.7 nM, respectively). Replacing the benzyl (**6l**, K_I of 248.3 nM) or anthryl (**6n**, K_I of 176.6 nM) rings with naphthalene ring in **6m** (K_I of 63.3 nM) significantly increased the inhibitory effect versus *h*CA II as in *h*CA I. Additionally, propargyl **6i** (K_I of 159.1 nM) exhibited an equipotent activity relative to the acetylamide **6j** derivative (K_I of 159.0 nM).

The ethyl derivative **6b** showed potent inhibitory effect with a K_I of 228.0 nM against the tumor-associated isoform *h*CA IX, and the replacement of a substituent, such as a nonyl group (**6f**, K_I of 200.7 nM) or a heptyl group (**6e**, K_I of 195.9 nM) increased the inhibitory action. In contrast, the pentyl (**6d**, K_I of 298.3 nM), propyl (**6c**, K_I of 394.4 nM), and methyl (**6a**, K_I of 660.0 nM) groups led to a reduction in activity. The presence of propargyl (**6i**), n-butenyl (**6h**), and acetylamide (**6j**) led to a considerable decrease in activity (K_Is of 443.0, 456.3, and 1072 nM, respectively). Furthermore, the replacement of the anthryl group (**6n**, K_I of 297.9 nM) with a benzyl group (**6l**, K_I of 528.0 nM) or with a naphthyl

group (**6m**, K_I of 704.8 nM) reduced the inhibitory effect.

As previously noted in relation to *h*CA IX, the kinetic profile of this compound series for the *h*CA XII isoform did not demonstrate significant differences and was largely similar. Remarkably, having the linear alkyl chains such as in methyl **6a**, ethyl **6b**, and propyl **6c** derivatives or elongation by these chains resulted in an increase of affinity against the tumor-associated isoform *h*CA XII. For example, the heptyl derivative **6e** (K_I of 116.9 nM) resulted to be 2.9-fold more active than **6d** (K_I of 337.3 nM) as well as the nonyl derivative **6f** (K_I of 147.8 nM) was 2.3-fold more active than **6d**. When compared to naphtyl derivative **6m** (K_I of 120.8 nM), anthryl and benzyl bearing ether derivatives **6n** and **6l** (K_Is of 254.2 and 558.6 nM, respectively) importantly decreased inhibitory effect towards *h*CA XII. Furthermore, replacing the acetylamide (as in compound **6j**, K_I of 207.6 nM) with diethylacetylamide group led to a more potent *h*CA XII inhibition with K_I of 151.5 nM.

Their primary sequences in the active sites of *h*CAs resemble one another by >30 %. Regardless of the species, all the known *h*CAs generally possess rather big active sites divided into two distinct sides, one lined with hydrophobic residues and the other e with polar, hydrophilic ones. Here, SARs parameters exhibited that compounds with benzene rings are weak inhibitors as compared to aliphatic compounds.

2.4. Selectivity parameters of the target compounds

The *h*CAs are closely linked since their primary sequences resemble one another by >30 %. It is not easy to construct isoform-selective *h*CAIs since most of the sequence identity matches residues found in the active site of *h*CA isoforms [50]. Synthesized 1,2,3-triazole benzenesulfonamide substituted oxime ether derivatives (**6a-n**) developed notable selectivity versus the cytosolic *h*CA I and II isoforms over the transmembrane *h*CA IX and XII isoforms. The selectivity of the synthesized compounds towards the *h*CA isoforms was evaluated using the enzyme selectivity index (S_I), which is the ratio of the K_I values for *h*CA I and II to *h*CA IX and XII. The S_I values, presented in Table 2, were used to determine the relative enzyme selectivity of the compounds.

Regarding selectivity towards *h*CA I over the isoform *h*CA IX, the determined S_I IX/I for 1,2,3-triazole benzenesulfonamide substituted oxime ethers (**6a-n**) were ranged from 10.3 to 1.7. Compound **6m** with a naphthyl showed high selectivity towards *h*CA I. The electron-donating groups, such as acetylamide **6j** and methyl **6a** derivatives, mainly decreased the selectivity with listed lower S_Is of 5.5 and 5.3, respectively. Also, the presence of the diethylacetylamide group on **6k** moderately reduced the selectivity (S_I of 3.1) relative to the acetylamide substituted **6j**. Replacement of the naphthyl group with another lipophilic benzyl or anthryl group in **6l** and **6n** also decreased the selectivity (S_Is of 2.0 and 1.8, respectively).

The selectivity of the 1,2,3-triazole benzenesulfonamide substituted oxime ether compounds (**6a-n**) towards *h*CA II over *h*CA IX was evaluated by calculating the enzyme S_I based on the K_I values presented in Table 2. The target compounds displayed high potency towards *h*CA II, with S_I IX/II values ranging from 11.7 to 1.7. Compound **6a**, featuring a methyl group, showed the highest selectivity towards *h*CA II, with an S_I of 11.7. However, modifications to the structure of **6a** led to decreased selectivity. Replacing the methyl group with a lipophilic naphthyl group in **6m**, and linear alkyl chains such as propyl in **6c** and ethyl in **6b**, resulted in decreased selectivity, with S_Is of 11.1, 9.8, and 6.9, respectively. Additionally, the presence of the diethylacetylamide moiety in **6k** (S_I of 6.7) led to a decline in selectivity compared to the acetylamide-substituted **6j** (S_I of 3.4).

Concerning selectivity towards *h*CA I over the isoform *h*CA XII, the calculated S_I XII/I for 1,2,3-triazole benzenesulfonamide substituted oxime ether derivatives (**6a-n**) ranged from 2.7 to 1.1. Derivative **6c** with a propyl group displayed a high selectivity against *h*CA I, S_I of 2.7. Replacement of the propyl group (**6c**) with linear alkyl chains, such as ethyl in **6b**, heptyl in **6e**, and methyl in **6a**, slightly decreased the selectivity (S_Is of 2.5, 2.4, and 2.3, respectively). Furthermore, replacing of the benzyl group in **6l** (S_I of 2.2) with a naphthyl group in **6m** (S_I of 1.8) or anthryl group **6n** (S_I of 1.5) also declined the selectivity. Also, the presence of the diethylacetylamide group on **6k** increased the selectivity relative to the acetylamide substituted **6j** with S_Is of 1.9 and 1.1, respectively.

In relation to selectivity towards *h*CA II over the isoform *h*CA XII, 1,2,3-triazole based benzenesulfonamide derivatives **6a-n** exhibited selectivity with S_I XII/II from 6.6 to 1.3. The presence of electron-donating groups like the pentyl in **6d**, propyl in **6c**, ethyl in **6b**, and methyl in **6a** showed the highest selectivity towards *h*CA II with S_Is of 6.6, 6.4, 5.8, and 5.0, respectively. The presence of the diethylacetylamide group on **6k** (S_I of 2.0) increased the selectivity relative to the acetylamide substituted **6j** (S_I of 1.3). Moreover, replacement of the benzyl group (**6l**, S_I of 2.2) with a more lipophilic groups, such as naphthyl in **6m** or anthryl in **6n** declined the selectivity (S_I of 1.9 and 1.4, respectively).

In summary, the results of this study demonstrate the strong impact of structural modifications on the selectivity profile of *h*CAs, leading to the development of highly selective drug candidates. The naphthyl (**6m**) and methyl (**6a**) derivatives exhibited the best selectivity towards *h*CA IX, while the propyl (**6c**) and pentyl (**6d**) derivatives were highly selective towards *h*CA XII. The most potent compounds, **6e** (K_I of 47.8 nM for *h*CA I) and **6b** (K_I of 33.2 nM for *h*CA II), showed good selectivity with S_Is of 4.1 and 2.5 (*h*CA I over *h*CAs IX and XII, respectively) and 3.0 and 5.8 (*h*CA II over *h*CAs IX and XII, respectively).

2.5. Cytotoxic activity of the target compounds

Based on the inhibition data of *h*CA IX and XII isoforms, a drug target for various cancer types, the selected most active 1,2,3-triazole benzenesulfonamide substituted oxime ethers (**6b**, **6e**, **6f**, **6g**, and **6k**) were investigated in terms of cytotoxic activity against some cell lines, human breast adenocarcinoma (MCF-7), human liver adenocarcinoma (Hep—3B), and normal mouse fibroblast (L929). Doxorubicin (DOX, PubChem CID: 31703), a clinically used drug, was included in the experiments as a reference inhibitor. Additionally, the selectivity index for cell line ($S_I^{(cell\ line)}$) was also calculated to evaluate these derivatives as potential anticancer agents. Here, agents with a selectivity index higher than 1 were regarded as selective against cancer cells [51] (Table 3).

Table 3
The cytotoxic activity and selectivity data of some 1,2,3-triazole benzenesulfonamide substituted oxime ethers and the reference inhibitor doxorubicin, a clinically used drug on normal mouse fibroblast (L929), human breast adenocarcinoma (MCF-7), and human liver adenocarcinoma (Hep—3B) cell lines using the MTT assay.

Compounds ID	IC_{50}[a] (μM)			$S_I^{(MCF-7)}$[b]	$S_I^{(Hep—3B)}$[b]
	L929	MCF-7	Hep-3B		
6b	19.0 ± 0.1	57.4 ± 0.1	24.5 ± 0.1	0.3	0.8
6e	591.1 ± 0.3	23.0 ± 0.1	47.2 ± 0.1	25.7	12.5
6f	142.3 ± 0.2	28.3 ± 0.1	ND[d]	5.0	ND[d]
6g	ND[d]	50.1 ± 0.1	533 ± 0.7	ND[d]	ND[d]
6k	52.3 ± 0.3	0.01 ± 0.001	1950 ± 3.2	5230	0.03
DOX[c]	96.9 ± 0.1	14.9 ± 0.1	11.1 ± 0.6	6.5	8.7

[a] IC_{50} values are the concentration of the compound that reduces the cell viability to 50 %, measured at 24 h of continuous exposure. The analysis results were expressed as means of triplicate assays ± SEM.
[b] The selectivity index for cell line ($S_I^{(cell\ line)}$): (IC_{50} for normal cell line L929)/(IC_{50} for respective cancerous cell line).
[c] Doxorubicin.
[d] Not determined.

Concerning activity towards breast cancer MCF-7 cells, diethylacetylamide derivative **6k** emerged as the most cytotoxic agent among these compounds, showing the lowest IC_{50} of 1.2 μM in this series better than that of the reference drug DOX (IC_{50} of 14.9 μM). Moreover, the heptyl (**6e**, IC_{50} of 23.0 μM) and nonyl (**6f**, IC_{50} of 28.3 μM) derivatives exhibited moderate activity against MCF-7 cells. On the other hand, ethyl **6b** and heptyl **6e** derivatives showed moderate anticancer activity against Hep-3B cells. However, none of the compounds were as active as DOX for Hep-3B cell lines. Additionally, these derivatives were compared to determine their cytotoxic profile against normal mouse fibroblast L929, the healthy cell line. Except for **6b** and **6k** from the tested compounds (**6b**, **6e**, **6f**, **6g**, and **6k**), others (**6e**, **6f**, and **6g**) were safe against L929 cells compared to standard drug DOX (IC_{50} of 96.9 μM) and were non-toxic. Given the above $S_I^{(\text{cell line})}$ index, derivative **6k** for MCF-7 (S_I of 43.6) and derivative **6e** for both cell lines, MCF-7 and Hep-3B (S_Is of 25.7 and 12.5, respectively) selectively inhibited the growth of cancerous cells compared to healthy cells. Based on the IC_{50} values and noticeable selectivity, heptyl **6e** and diethylacetylamide **6k** derivatives may be recommended for further investigation of their mechanism of cytotoxic action on various cancer cell lines.

2.6. In silico study

The binding patterns of 1,2,3-triazole benzenesulfonamide substituted oxime ethers (**6a-n**), synthesized in this study, were investigated using X-ray crystallographic structures of *h*CA I (PDB ID 1AZM) [52], *h*CA II (PDB ID 3HS4) [53], *h*CA IX (PDB ID 3IAI) [54], and *h*CA XII (PDB ID 1JD0) [55] isoforms. The docking setup was validated by re-docking the co-crystallized native ligand AZM (AAZ, 5-acetamido-1,3,4-thiadiazole-2-sulfonamide) into the enzyme binding sites. The docking methodology was deemed reliable, as evidenced by minimal RMSD values (0.21, 1.02, 1.29, and 1.33 for 1AZM, 3HS4, 3IAI, and 1JD0, respectively) and the ability of the docking poses of the co-crystalized ligands to reproduce all essential interactions.

The binding patterns were tested using a validated docking setup, and the most potent inhibitors, **6e** (for *h*CA I, IX, and XII isoforms) and **6b** (for *h*CA II isoform), were found to exhibit strong binding affinity with predicted docking scores in the range of −1.71 to −6.33 kcal/mol and MM-GBSA values of −13.26 to 30.33 kcal/mol. The binding patterns of the synthesized agents in the *h*CA isoforms showed comparable accommodation of the sulfonamide moiety deeply in the active site, interacting with the zinc-ion, and by hydrogen bonding with gatekeeper residues, such as Thr199 and Thr200. The triazole moiety was involved in hydrogen bonding and pi-pi stacking interactions with specific residues, such as Trp5 in *h*CA IX, while the benzenesulfonamide phenyl ring interacted through pi-pi stacking with polar residue His94 in *h*CA XII. Furthermore, the 1,2,3-triazole moiety showed hydrophobic interaction with Phe91 in *h*CA I, Phe131 in *h*CA II, and Trp5 in *h*CA IX isoform (Figs. 2-5). The novel synthesized agents displayed varying binding affinity and selectivity patterns in each *h*CA isoform, which could be attributed to the different structural modifications that imparted various steric and electronic properties. Therefore, the present study provides valuable insights into the binding mechanisms of the 1,2,3-triazole benzenesulfonamide substituted oxime ethers in *h*CA isoforms and highlights their potential as selective drug candidates for the treatment of diseases associated with carbonic anhydrase dysfunction.

Additionally, using the QikProp module of the Schrödinger Suite 2022–3 for Mac, the chemical drug-likeness of the targeted novel 1,2,3-triazole benzenesulfonamide substituted oxime ethers (**6a-n**) was evaluated. The relevant ADME/T (absorption, distribution, metabolism, elimination, and toxicity) parameters were calculated and subsequently presented in Table 4. Based on physicochemical characteristics, it is evident that the oxime ethers under examination exhibited drug-like characteristics, and all of the derivatives (**6a-n**) adhere to Lipinski's five [56], Jorgensen's three [57] rules and PAINS alert [58].

3. Conclusion

In the present study, a novel series of 1,2,3-triazole benzenesulfonamide substituted oxime ethers (**6a-n**) were synthesized using the tail method. The molecular hybridization strategy was employed to combine the zinc-binding 4-benzenesulfonamide moiety with the 1,2,3-triazole scaffold. The hydrophobic tail was constructed using the oxime moiety. The inhibitory potential of these derivatives was evaluated against four isoforms of α-*h*CA, namely *h*CA I, II, IX, and XII. Compared to AAZ, compound **6e** (K_Is of 47.8, 195.9, and 116.9 nM, respectively) had significantly more potent inhibitory action against cytosolic isoform *h*CA I and tumor-associated isoforms *h*CA IX and hCA XII. Another cytosolic isoform *h*CA II was more effectively inhibited by ethyl derivative **6b** (K_I of 33.2 nM) than by AAZ (K_I of 327.3 nM). The naphtyl (**6m**, S_I of 10.3), and methyl (**6a**, S_I of 11.7) derivatives (over *h*CA IX) and propyl (**6c**, S_I of 2.7), and pentyl (**6d**, S_I of 6.6) derivatives (over *h*CA XII) exhibited a remarkable selectivity for isoforms *h*CA I and II, respectively. Additionally, adding the lipophilic large naphthyl tail to the 1,2,3-triazole benzenesulfonamide substituted oxime ether derivatives increased inhibitory effect versus *h*CA I and XII and selectivity towards *h*CA I and II isoforms over *h*CA IX. Cytotoxic screening in L929, MCF-7, and Hep-3B cells identified heptyl (**6e**, IC_{50}s of 591.1, 23.0, and 47.2 μM, respectively) and diethylacetylamide (**6k**, IC_{50}s of 52.3, 0.01, and 1950 μM, respectively) derivatives with good antiproliferative activity and low cytotoxicity. Moreover, the present study employed molecular docking techniques to investigate the binding of these compounds (**6a-n**) within the active sites of *h*CAs. The results revealed that the sulfonamide moiety was accommodated deeply in the active site and interacted with the zinc-ion within the binding site. Furthermore, the sulfonamide moiety formed hydrogen bonds with the crucial residue Thr199, indicating the significance of this residue in the binding process.

4. Experimental section

4.1. General procedure for the preparation of the target compounds

All the chemicals and solvents used during the study were purchased from Sigma-Aldrich and used without further purification. Melting points were determined by Yanagimoto micro-melting point apparatus and uncorrected. Infrared (IR) spectra were measured on a Shimadzu Prestige-21 (200 VCE) spectrometer. ^{1}H and ^{13}C NMR spectra were obtained using VARIAN Infinity Plus at 300 and 75 Hz, respectively. ^{1}H and ^{13}C chemical shifts were referenced to the internal deuterated solvent. Mass spectra were measured on a 6200 series TOF/6500 series Q-TOF B.08.00 (B8058.0) spectrometer.

4.1.1. General procedure for preparation of 4-azidobenzenesulfanilamide (3)

Sulfanilamide (**1**) (0.5 g, 3 mmol) was dissolved in H_2O and 6 M HCl (10 mL) and cooled to 0 °C. Sodium nitrite (248 mg, 3.6 mmol) dissolved in 15 mL of cold water was added dropwise to the mixture and stirred continuously for 25 min at 0 °C. At the end of this step, sulfonilamide diazonium salt was prepared. Then, Sodium azide (282 mg, 4.4 mmol) was added to the solution containing diazonium salt and continued to stir for 2 h more at room temperature to give the corresponding azido derivative (**3**). The final product was washed with water, collected by filtration, and dried. The compound was used for the next step without further purification.

4.1.2. General procedure for preparation of 1,2,3-triazole benzenesulfonamide (4)

A solution of azido benzenesulfonamide (1 mmol) in DMF has added acetylacetone (1.5 mmol) using potassium carbonate (2 mmol) as a base at 80 °C refluxing with continuous stirring for 5–6 h. At the end of the reaction, the mixture was extracted with ethyl acetate and washed with 1 M sodium hydroxide solution, saturated $NaHCO_3$ solution, and brine.

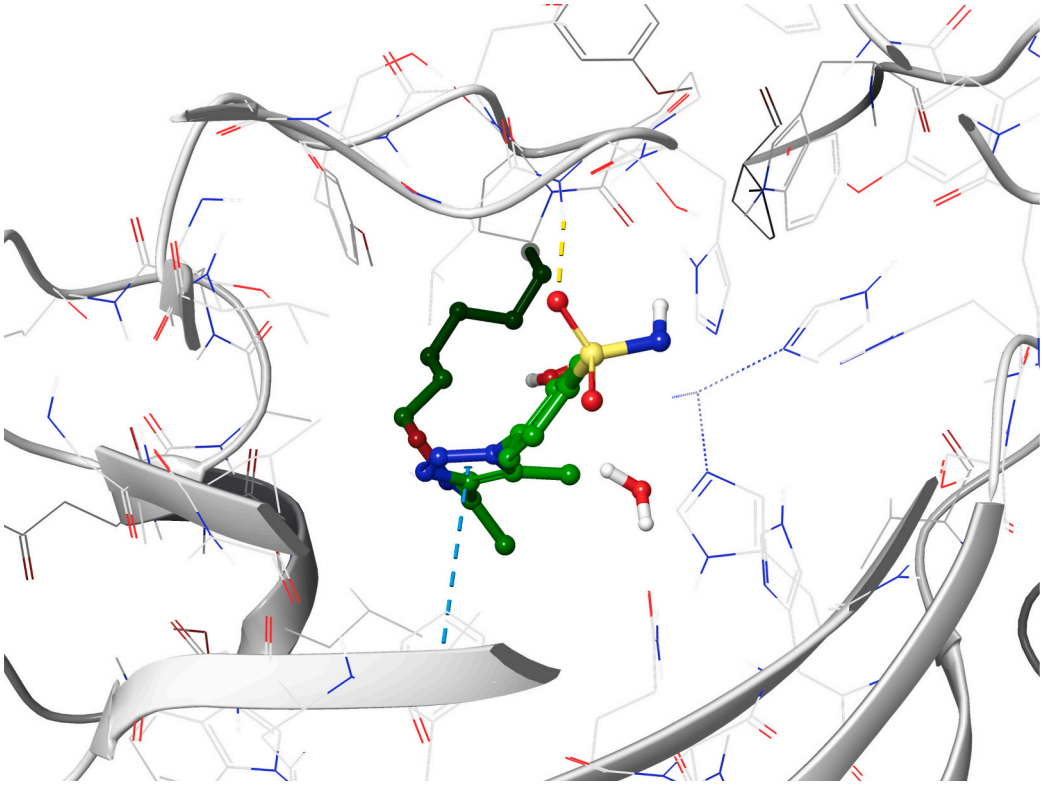

A

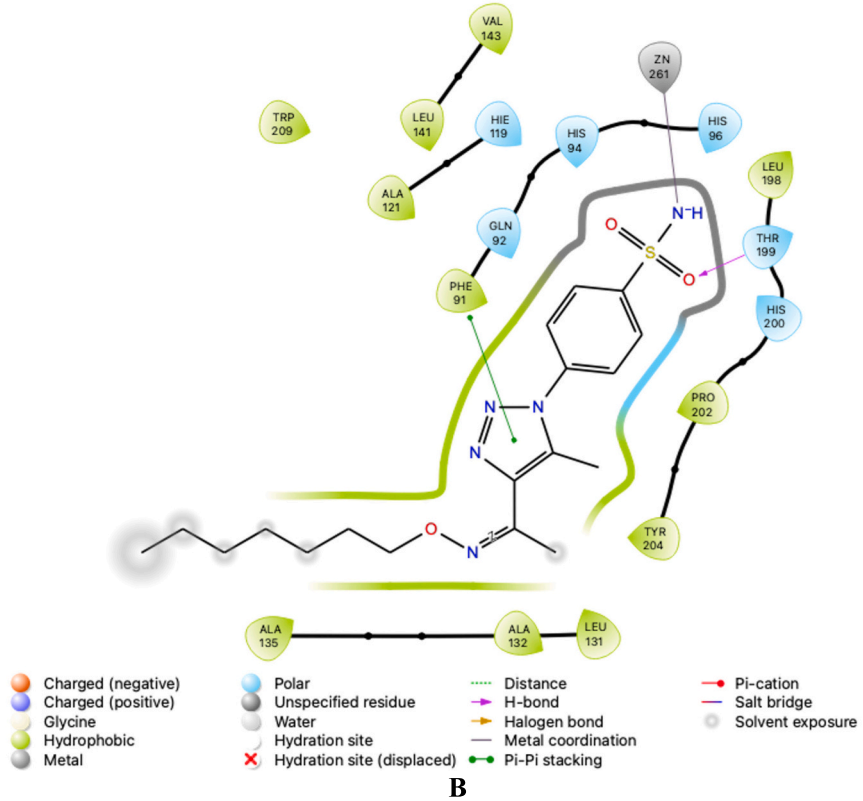

B

Fig. 2. Molecular docking of *h*CA I isoform (PDB ID 1AZM) with 4-(4-{1-[(heptyloxy)imino]ethyl}-5-methyl-1*H*-1,2,3-triazol-1-yl)benzenesulfonamide (**6e**). (A) 3D docking pose of derivative **6e** within the binding pocket of 1AZM. In the 3D panel, hydrogen bonds and pi-pi stacking interactions are shown in yellow and blue dashed lines, respectively. Only the interacting amino acids are demonstrated for the sake of clarity. (B) 2D interaction diagram of 1AZM with derivative **6e**. (For interpretation of the references to colour in this figure legend, the reader is referred to the web version of this article.)

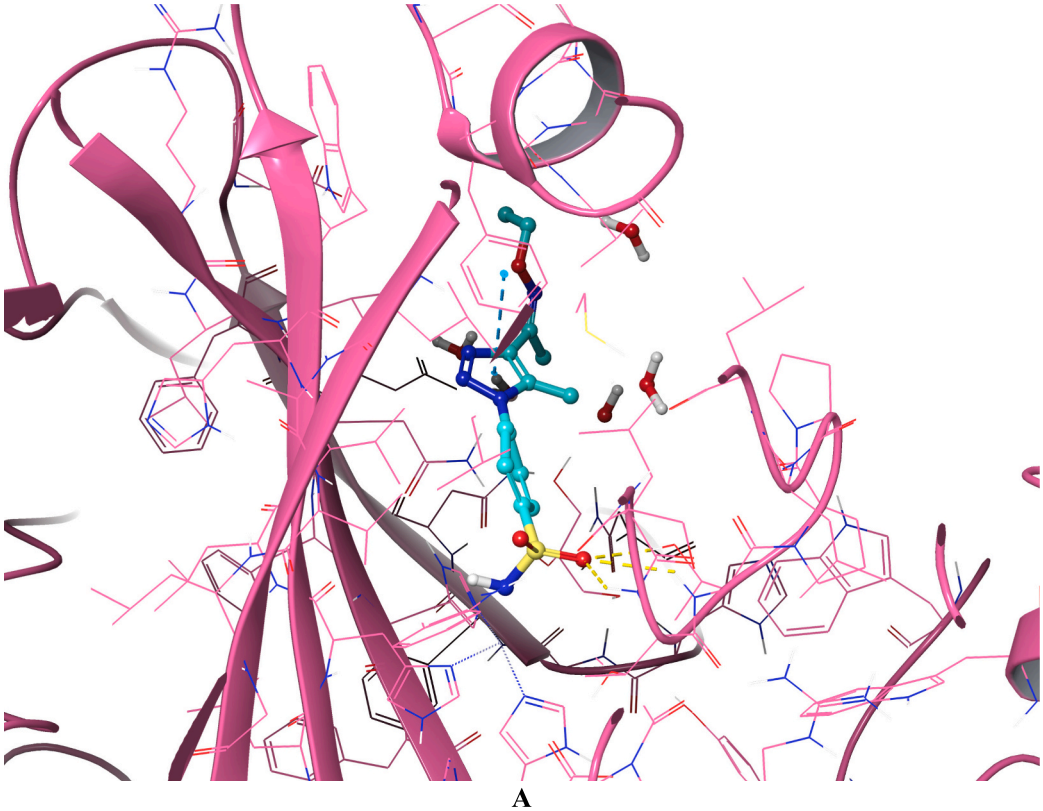

A

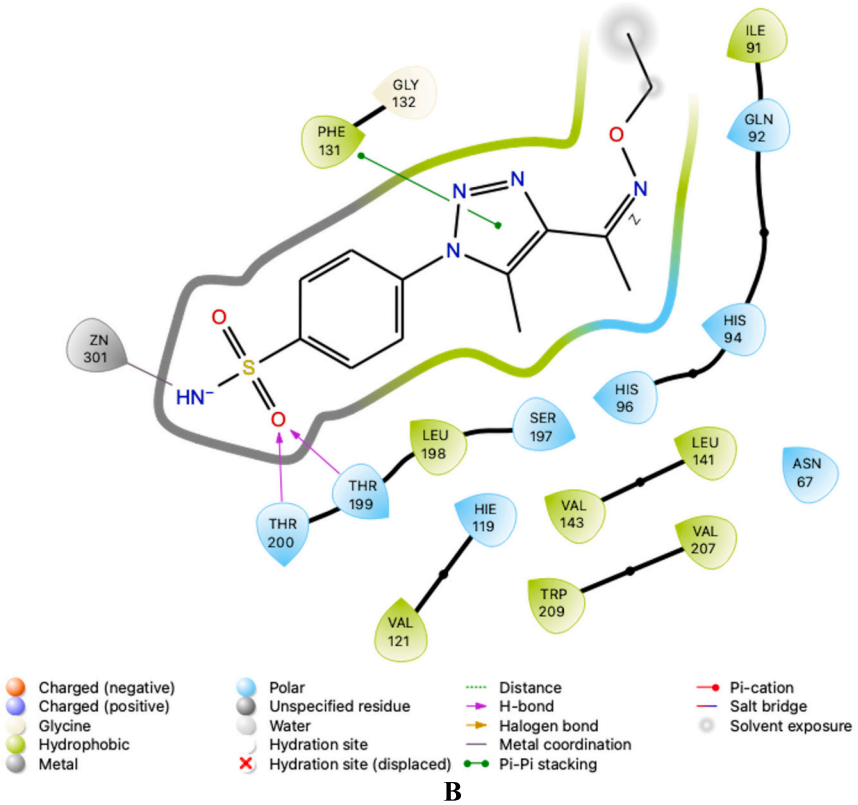

B

Fig. 3. Molecular docking of *h*CA II isoform (PDB ID 3HS4) with 4-{4-[1-(ethoxyimino)ethyl]-5-methyl-1*H*-1,2,3-triazol-1-yl}benzenesulfonamide (**6b**). (A) 3D docking pose of derivative **6b** within the binding pocket of 3HS4. In the 3D panel, hydrogen bonds and pi-pi stacking interactions are shown in yellow and blue dashed lines, respectively. Only the interacting amino acids are demonstrated for the sake of clarity. (B) 2D interaction diagram of 3HS4 with derivative **6b**. (For interpretation of the references to colour in this figure legend, the reader is referred to the web version of this article.)

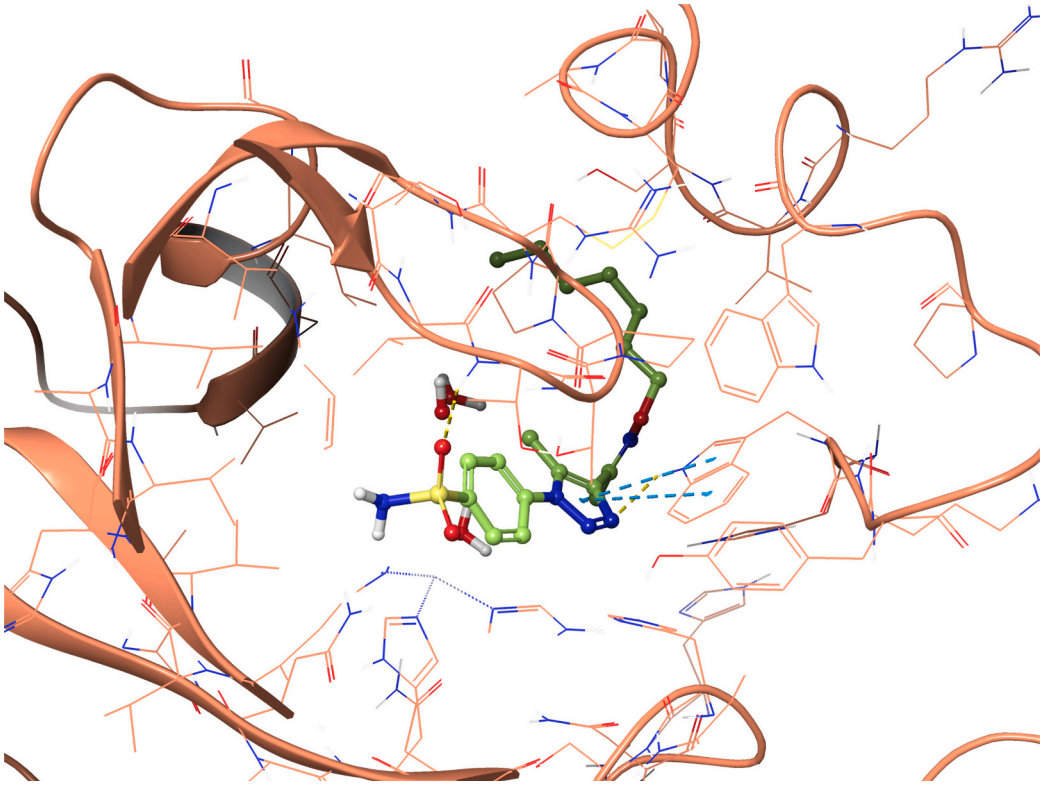

A

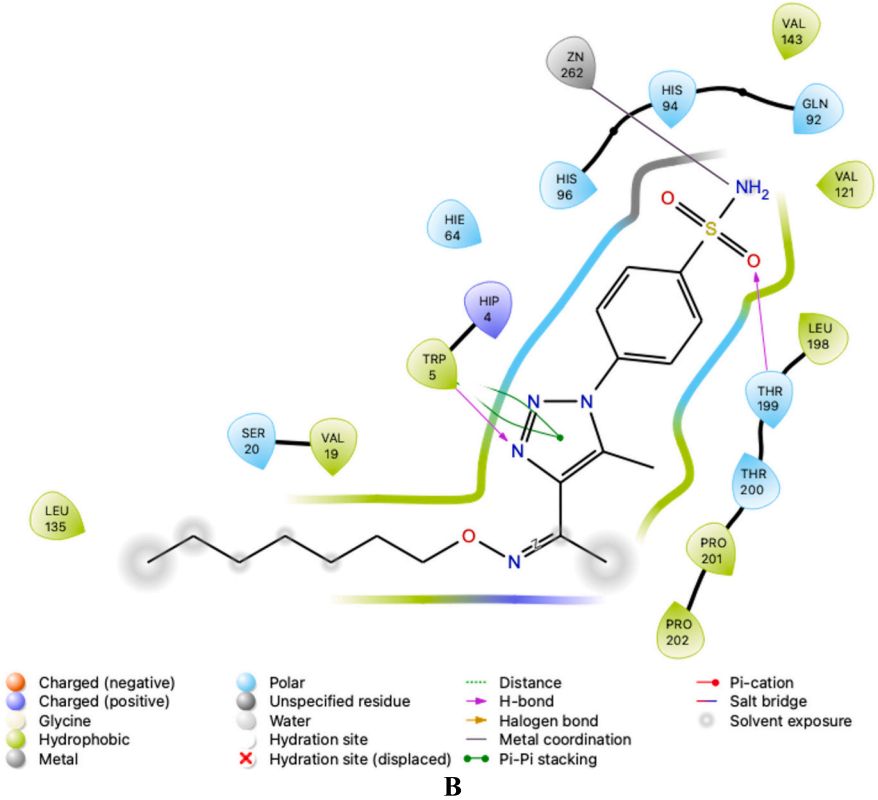

B

Fig. 4. Molecular docking of *h*CA IX isoform (PDB ID 3IAI) with 4-(4-{1-[(heptyloxy)imino]ethyl}-5-methyl-1*H*-1,2,3-triazol-1-yl)benzenesulfonamide (**6e**). (A) 3D docking pose of derivative **6e** within the binding pocket of 3IAI. In the 3D panel, hydrogen bonds and pi-pi stacking interactions are shown in yellow and blue dashed lines, respectively. Only the interacting amino acids are demonstrated for the sake of clarity. (B) 2D interaction diagram of 3IAI with derivative **6e**. (For interpretation of the references to colour in this figure legend, the reader is referred to the web version of this article.)

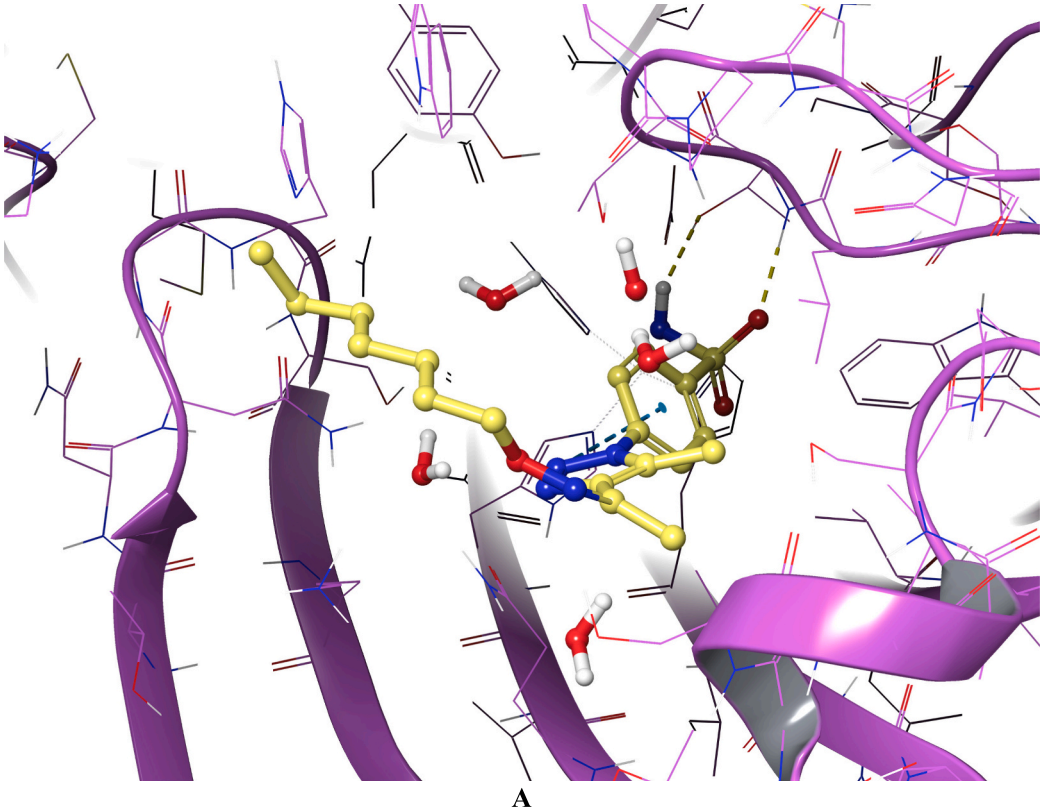

A

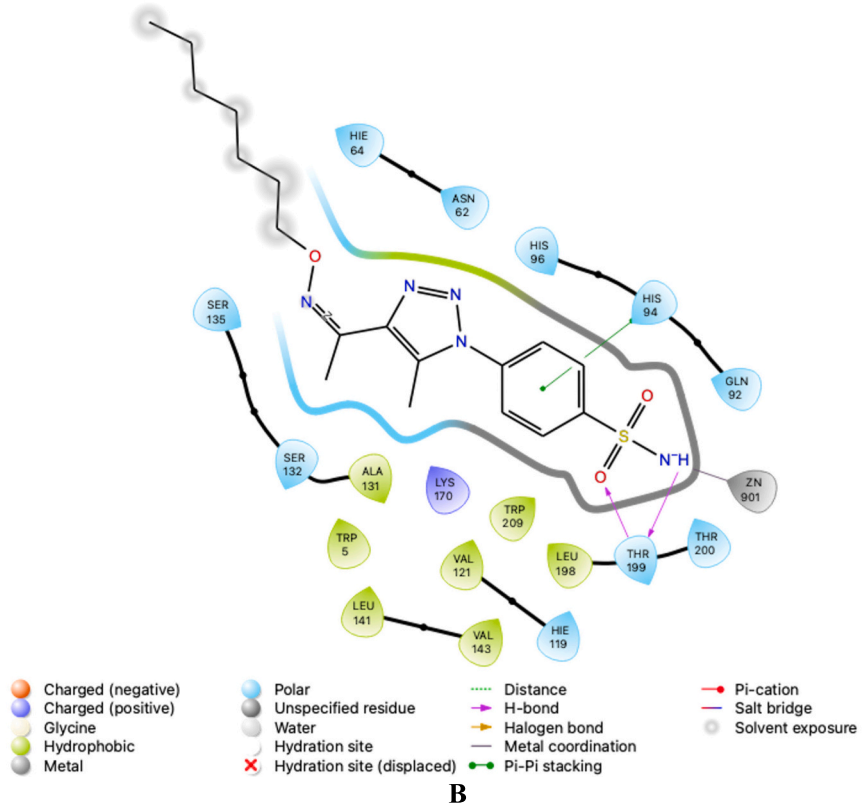

B

Fig. 5. Molecular docking of *h*CA XII isoform (PDB ID 1JD0) with 4-(4-{1-[(heptyloxy)imino]ethyl}-5-methyl-1*H*-1,2,3-triazol-1-yl)benzenesulfonamide (**6e**). (A) 3D docking pose of derivative **6e** within the binding pocket of 1JD0. In the 3D panel, hydrogen bonds and pi-pi stacking interactions are shown in yellow and blue dashed lines, respectively. Only the interacting amino acids are demonstrated for the sake of clarity. (B) 2D interaction diagram of 1JD0 with derivative **6e**. (For interpretation of the references to colour in this figure legend, the reader is referred to the web version of this article.)

Table 4
ADME-Tox related parameters [a] of novel synthesized 1,2,3-triazole benzenesulfonamide substituted oxime ethers (**6a-n**) and the reference inhibitor acetazolamide, a clinically used drug.

Compounds ID	MW	Dipole	Volume	QPlogPoct	QPlogPw	QPlogPo/w	QPlogS	QPPCaco	QPlogBB	QPPMDCK	QPlogKp	QPlogKhsa	HOA	PSA	Rule of Five	Rule of Three	PAINS
6a	309.34	10.20	963.06	19.31	14.29	0.23	−2.92	106.43	−1.78	44.78	−4.41	−0.64	64.55	117.86	0	0	0
6b	323.37	1.64	1027.84	18.44	14.09	0.63	−3.29	121.71	−1.84	51.84	−4.21	−0.56	67.97	117.68	0	0	0
6c	337.40	10.10	1083.44	20.18	13.87	0.99	−3.50	135.05	−1.87	58.00	−4.03	−0.47	70.86	117.01	0	0	0
6d	365.45	1.18	1292.47	20.09	13.67	1.69	−4.36	125.16	−2.18	53.38	−3.89	−0.29	74.40	117.26	0	0	0
6e	393.50	10.02	1327.85	22.18	13.32	2.42	−5.03	134.70	−2.35	57.85	−3.65	−0.88	79.24	116.96	0	0	0
6f	421.56	3.88	1292.47	20.42	12.25	2.32	−3.07	171.03	−1.89	74.46	−3.42	−0.17	80.52	115.39	0	0	0
6g	335.38	10.08	1072.58	20.27	14.26	0.93	−3.53	117.21	−1.97	49.79	−3.98	−0.51	69.40	117.79	0	0	0
6h	349.41	10.15	1133.39	20.78	14.11	1.29	−3.88	122.17	−2.07	52.03	−3.85	−0.42	71.87	117.52	0	0	0
6i	333.36	4.29	1047.48	19.69	15.10	0.75	−3.41	113.65	−1.98	48.25	−3.94	−0.55	68.13	117.95	0	0	0
6j	352.37	9.53	1054.05	24.46	22.23	−1.60	−1.81	7.75	−2.90	4.84	−5.96	−1.16	33.49	171.15	0	1	0
6k	408.47	6.85	1259.19	23.10	18.99	0.80	−2.28	48.22	−2.22	35.23	−4.23	−1.00	57.54	143.98	0	0	0
6l	385.44	8.66	1203.81	22.35	15.36	1.92	−4.50	134.82	−1.97	57.90	−3.34	−0.20	76.31	116.57	0	0	0
6m	435.50	5.80	1310.66	23.56	15.61	2.75	−4.97	192.85	−1.73	85.27	−2.89	0.76	83.94	116.10	0	0	0
6n	485.56	9.37	1447.13	26.32	16.38	1.3.64	−6.19	176.84	−−1.89	77.63	−2.67	0.40	88.46	117.16	0	1	0
AAZ[b]	222.24	10.76	634.43	17.57	15.15	−1.75	−1.55	36.88	−1.74	24.13	−5.90	−0.97	44.77	134.97	0	0	0

[a] Various computational pharmacodynamic and pharmacokinetic parameters of synthesized compounds in this research were predicted such as molecular weight of the compound (MW; 130.00–725.00), computed dipole moment of the compound (Dipole; 1.00–12.50), total solvent-accessible volume in cubic angstroms using a probe with a 1.4 Å Radius (Volume; 500.00–2000.00), octanol/gas partition coefficient (QPlogPoct; 8.00–35.00), water/gas partition coefficient (QPlogPw; 4.00–45.00), octanol/water partition coefficient (QPlogPo/w; −2.00 - 6.50), aqueous solubility (QPlogS; −6.50 - 0.50), apparent Caco-2 cell permeability in nm/s (QPPCaco; <25 poor, great>500), brain/blood partition coefficient (QPlogBB; −3.00 - 1.20), apparent MDCK cell permeability in nm/s (QPPMDCK; <25 poor, great>500), skin permeability (QPlogKp; −8.00 - −1.00), prediction of binding to human serum albumin (QPlogKhsa; −1.50 - 1.50), human oral absorption (HOA; <25 % poor, high>80 %), van der Waals surface area of polar nitrogen and oxygen atoms (PSA; 7.00–200.00), number of violations of Lipinski's rule of five (max. 4), number of violations of Jorgensen's rule of three (max. 3), and pan-assay interference compounds (PAINS) alert.

[b] Acetazolamide.

The organic phase was dried over $MgSO_4$, filtered, and evaporated under a vacuum. The product was purified by crystallization from $CHCl_3$. 1,2,3-Triazole benzenesulfonamide derivative (**4**) was obtained as pure.

4.1.3. General procedure for preparation of oxime derivatives (5)

Hydroxylamine hydrochloride (3 mmol) was added to 4-(4-acetyl-5-methyl-1*H*-1,2,3-triazol-1-yl)benzenesulfonamide (1 mmol) (**4**) preliminarily dissolved in DMF, added a few drops Et_3N as a catalyst, and the mixture continued to stir at 100 °C for 10 h to give the corresponding oxime derivative (**5**). The reaction mixture was cooled to room temperature, and ice-cold water was added, then filtered and dried. The oxime derivative, (*E*)-4-{4-[1-(hydroxyimino)ethyl]-5-methyl-1*H*-1,2,3-triazol-1-yl}benzenesulfonamide (**5**) was purified by crystallization from acetone-hexane.

4.1.4. General procedure for preparation of targeted compounds *6a-n*

In the final step, the oxime derivative reacted with a stoichiometric amount of different alkyl, aryl, and benzyl halides in the presence of NaOH as a base, DMSO as a solvent, and TBAB as a phase transfer catalyst to give corresponding substituted oxime ether compounds with 1,2,3-triazole benzenesulfonamide (**6**, (*E*)-4-{4-[1-(hydroxyimino) ethyl]-5-methyl-1*H*-1,2,3-triazol-1-yl}benzenesulfonamide). At the end of the reaction, ice-cold water was added to the flask and then filtered and dried. The final targeted products (**6a-n**) were purified by crystallization from acetone-hexane. The prepared compounds shown in Scheme 1 were characterized by ^{1}H NMR, ^{13}C NMR, IR, and mass analysis.

4.1.4.1. 4-{4-[1-(Methoxyimino)ethyl]-5-methyl-1H-1,2,3-triazol-1-yl} benzenesulfonamide (6a). Yield 79 %; m.p.166 °C; IR (υ, cm^{-1}): 3350 (N—H), 2990 (C—H), 1505 (C=C), 1348 and 1163 (SO_2); ^{1}H NMR (300 MHz, DMSO-d_6, ppm): 7.86–8.05 (4H, d, -Ar-H), 7.59 (2H, s-NH_2), 3.91 (3H, s, -CH_3), 2.49 (3H, s, -CH_3), 2.30 (3H, s, -CH_3); ^{13}C NMR (75 MHz, DMSO-d_6, ppm): 145.6, 141.1, 138.5, 131.9, 129.3, 127.8, 126.01, 124.6 (2C), 74.6, 11.1, 13.3; $C_{12}H_{15}N_5O_3SH^+$: (ES-API, pos. ion): (M + 1) m/z = 310.0968, calcd. For 310.0974

4.1.4.2. 4-{4-[1-(Ethoxyimino)ethyl]-5-methyl-1H-1,2,3-triazol-1-yl}benzenesulfonamide (6b). Yield 75 %; m.p. 149 °C; IR (υ, cm^{-1}): 3369 (N—H), 2982 (C—H sp^3), 1505 (C=C), 1350 and 1165 (SO_2); ^{1}H NMR (300 MHz, DMSO-d_6, ppm): 7.61 (2H, s-NH_2), 7.89–8.02 (4H, d, -Ar-H), 4.12–4.17 (2H, q, -CH_2), 3.37 (3H, s, -CH_3), 2.3 (3H, s, -CH_3), 1.24–1.28 (3H, t, -CH_3); ^{13}C NMR (75 MHz, DMSO-d_6, ppm): 150.1, 145.6, 141.4, 138.6, 133.1, 127.8 (2C), 126.5 (2C), 69.8, 15.3, 13.3, 11.14; $C_{13}H_{17}N_5O_3SH^+$: (ES-API, pos. ion): (M + 1) m/z = 324.1124, calcd. For 324.1130

4.1.4.3. 4-{5-Methyl-4-[1-(propoxyimino)ethyl]-1H-1,2,3-triazol-1-yl} benzenesulfonamide (6c). Yield 81 %; m.p.186 °C; 3352 (N—H), 2992 (C—H sp^3), 1505 (C=C), 1355 and 1105 (SO_2); ^{1}H NMR (300 MHz, DMSO-d_6, ppm): 7.85–8.05 (4H, d, -Ar-H), 7.59 (2H, s-NH_2), 4.05–4.09 (2H, t, -CH_2), 2.31 (3H, s, -CH_3), 2.49 (3H, s, -CH_3), 0.88–0.93 (3H, t, -CH_3), 1.68 (2H, m, -CH_2); ^{13}C NMR (75 MHz, DMSO-d_6, ppm): 150.1, 145.6, 141.3, 138.6, 133.1, 128.6, 127.8 (2C), 126.4 (2C), 75.7, 22.7, 13.2, 11.1; $C_{14}H_{19}N_5O_3SH^+$: (ES-API, pos. ion): (M + 1) m/z = 338.1281, calcd. For 338.1287

4.1.4.4. 4-(5-Methyl-4-{1-[(pentyloxy)imino]ethyl}-1H-1,2,3-triazol-1-yl)benzenesulfonamide (6d). Yield 81 %; m.p.152 °C; IR (υ, cm^{-1}): 3373 (N—H), 2878 (C—H sp^3), 1543 (C=C), 1505 (C=N), 1345 and 1165 (SO_2); ^{1}H NMR (300 MHz, DMSO-d_6, ppm): 7.87–8.05 (4H, d, -Ar-H), 7.62 (2H, s-NH_2), 4.08–4.13 (2H, t, -CH_2), 2.50 (3H, s, -CH_3), 2.30 (3H, s, -CH_3),1.31–1.34 (6H, m, -CH_2); 0.86–0.88 (3H, t, -CH_3), ^{13}C NMR (75 MHz, DMSO-d_6, ppm): 150.4, 145.6, 141.3, 138.6, 133.1, 127.8 (2C), 126.5 (2C), 74.3, 29.05, 28.3, 22.6, 14.6, 13.3, 11.1; $C_{16}H_{23}N_5O_3SH^+$:

(ES-API, pos. ion): (M + 1) *m/z* = 366.1594, calcd. For 366.1600

*4.1.4.5. 4-(4-{1-[(Heptyloxy)imino]ethyl}-5-methyl-1H-1,2,3-triazol-1-yl)benzenesulfonamide (**6e**).* Yield 79 %; m.p.126 °C; IR (υ, cm^{-1}): 3373 (N—H), 2878 (C—H sp^3), 1543 (C=C), 1347 and 1164 (SO_2); ^{1}H NMR (300 MHz, DMSO-d_6, ppm): 7.87–8.05 (4H, d, -Ar-H), 7.62 (2H, s, -NH_2), 4.15- (2H, t, -CH_2), 1.33–1.68(10H, m, -CH_2), 2.52 (3H, s, -CH_3), 2.09 (3H, s, -CH_3), 0.84–0.88(3H, t-CH_3); ^{13}C NMR (75 MHz, DMSO-d_6, ppm): 149.75, 145.49, 138.55, 132.30, 127.81 (2C), 125.69 (2C), 78.36, 74.42, 31.95, 29.28(2C), 26.10, 22.78, 14.49, 12.91, 11.24; $C_{18}H_{27}N_5O_3SH^+$: (ES-API, pos. ion): (M + 1) *m/z* = 394.1903, calcd. For 394.1913

*4.1.4.6. 4-(5-Methyl-4-{1-[(octyloxy)imino]ethyl}-1H-1,2,3-triazol-1-yl) benzenesulfonamide (**6f**).* Yield 88 %; m.p.174 °C; IR (υ, cm^{-1}): 3380 (N—H), 2875 (C—H sp^3), 1596 (C=N), 1540 (C=C), 1350 and 1164 (SO_2); ^{1}H NMR (300 MHz, DMSO-d_6, ppm): 7.87–8.05 (4H, d, -Ar-H),7.59 (2H, s-NH_2), 4.07–4.12 (2H, t, -CH_2), 2.50 (3H, s, -CH_3), 2.29 (3H, s, -CH_3), 1.25–1.66 (12H, m, -CH_2), 0.81–0.83 (3H, t, -CH_3); ^{13}C NMR (75 MHz, DMSO-d_6, ppm): 150.1, 145.6, 141.4, 138.6, 133.02, 127.8 (2C), 126.4 (2C), 74.3, 31.8, 29.4, 26.1 (2), 22.7, 14.6, 13.2, 11.1; $C_{19}H_{29}N_5O_3SH^+$: (ES-API, pos. ion): (M + 1) *m/z* = 408.2064, calcd. For 408.2069

*4.1.4.7. 4-(4-{1-[(Allyloxy)imino]ethyl}-5-methyl-1H-1,2,3-triazol-1-yl) benzenesulfonamide (**6g**).* Yield 85 %; m.p.175 °C; IR (υ, cm^{-1}): 3371 (N—H), 1648 (C=N); 1596 (C=C), 1350 and 1163 (SO_2); ^{1}H NMR (300 MHz, DMSO-d_6, ppm): 7.76–8.02 (4H, d, -Ar-H), 7.52 (2H, s-NH_2), 5.95–6.02 (1H, m = CH), 5.25–5.30 (1H, d, =CH), 5.16–5.19 (1H, d, =CH), 4.60–4.63 (2H, d, -CH_2), 3.37 (3H, s, -CH_3), 2.33 (3H, s, -CH_3); ^{13}C NMR (75 MHz, DMSO-d_6, ppm): 150.5, 145.6, 141.3, 138.5, 135.1, 132.8, 127.8 (2C), 126.1 (2C), 117.9, 78.9, 13.1, 11.2; $C_{14}H_{17}N_5O_3SH^+$: (ES-API, pos. ion): (M + 1) *m/z* = 336.1124, calcd. For 335.1130

*4.1.4.8. 4-(4-{1-[(But-3-en-1-yloxy)imino]ethyl}-5-methyl-1H-1,2,3-triazol-1-yl)benzenesulfonamide (**6h**).* Yield 79 %; m.p.135 °C; IR (υ, cm^{-1}): 3370 (N—H), 2937 (C—H sp^3), 1642 (C=N),1596 (C=C), 1355 and1162 (SO_2); ^{1}H NMR (300 MHz, DMSO-d_6, ppm): 7.88–8.05 (4H, d, -Ar-H), 7.61 (2H, s-NH_2), 5.82–5.91(1H, m, =CH), 5.08–5.13 (1H, d, =CH), 5.02–5.07 (1H, d, =CH), 4.16–4.19 (2H, t, -CH_2), 3.37 (3H, s, -CH_3), 2.41–2.52 (2H, q, -CH_2), 2.31-(3H, s, -CH_3); ^{13}C NMR (75 MHz, DMSO-d_6, ppm): 150.5, 145.6, 141.3, 138.6, 135.7, 133.1, 127.8 (2C), 126.5 (2C), 117.5, 73.4, 33.9, 13.3, 11.1; $C_{15}H_{19}N_5O_3SH^+$: (ES-API, pos. ion): (M + 1) *m/z* = 350.1282 calcd. For 350.1287

*4.1.4.9. 4-(5-Methyl-4-{1-[(prop-2-yn-1-yloxy)imino]ethyl}-1H-1,2,3-triazol-1-yl)benzenesulfonamide (**6i**).* Yield 95 %; m.p.118 °C; IR (υ, cm^{-1}): 3370 (N—H), 3300 (triplebond-H, stretch), 2937 (C—H sp^3), 1642 (C=N), 1596 (C=C), 1347 and 1160 (SO_2); ^{1}H NMR (300 MHz, DMSO-d_6, ppm): 7.90–8.07 (4H, d, -Ar-H), 7.63 (2H, s-NH2), 4.81 (2H, s, -CH_2), 3.52 (1H, s, ≡CH), 2.52 (3H, s, -CH_3), 2.35 (3H, s, -CH_3); ^{13}C NMR (75 MHz, DMSO-d_6, ppm): 151.7, 145.6, 140.9, 138.5, 133.5, 127.8 (2C), 126.5(2C), 81.1, 78.1, 62.1, 13.4, 11.1; $C_{14}H_{15}N_5O_3SH^+$: (ES-API, pos. ion): (M + 1) *m/z* = 334.0968, calcd. For 334.0974

*4.1.4.10. 2-[({1-[5-Methyl-1-(4-sulfamoylphenyl)-1H-1,2,3-triazol-4-yl] ethylidene}amino)oxy]acet amide (**6j**).* Yield 95 %; m.p.220 °C; IR (υ, cm^{-1}): 3318 (N—H), 1690 (C = 0), 1642 (C=N), 1598 (C=C), 1345 and1160 (SO_2); ^{1}H NMR (300 MHz, DMSO-d_6, ppm): 7.89–8.05 (4H, d, -Ar-H), 7.61 (2H, s-NH_2), 4.50 (2H, s, -CH_2), 3.37 (3H, s, -CH_3), 2.55 (3H, s, -CH_3), 2.28 (2H, s, -NH_2); ^{13}C NMR (75 MHz, DMSO-d_6, ppm): 11.1, 13.7, 73.3, 126.5, 171.7, 170.1, 152.0, 145.6, 141.0, 138.6, 133.4, 128.8, 127.8; $C_{13}H_{16}N_6O_4SH^+$: (ES-API, pos. ion): (M + 1) *m/z* = 353.1027, calcd. For 353.1032

*4.1.4.11. N,N-Diethyl-2-[({1-[5-methyl-1-(4-sulfamoylphenyl)-1H-1,2,3-triazol-4-yl]ethylidene}amino) oxy]acetamide (**6k**).* Yield 92 %; m.p.198 °C; IR (υ, cm^{-1}): 3271 (N—H), 1728 (C = O) 1499 (C=C,), 1345 and 1160 (SO_2); ^{1}H NMR (300 MHz, DMSO-d_6, ppm): 7.86–8.04 (4H, d, -Ar-H), 7.60 (2H, s-NH_2), 4.81 (2H, s, -CH_2), 3.28–3.31 (4H, q, -CH_2), 3.23 (3H, s, -CH_3), 2.07 (3H, s, -CH_3), 1.07–1.12 (6H, t, -CH_3); ^{13}C NMR (75 MHz, DMSO-d_6, ppm): 167.7, 151.1, 145.6, 141.1, 138.6, 133.4, 127.8 (2C), 126.4 (2C), 72.3, 41.2 (2C), 14.8 (2C), 13.5, 10.9; $C_{17}H_{24}N_6O_4SH^+$: (ES-API, pos. ion): (M + 1) *m/z* = 409.1653, calcd. For 409.1658

*4.1.4.12. N,N-Diethyl-2-[({1-[5-methyl-1-(4-sulfamoylphenyl)-1H-1,2,3-triazol-4-yl]ethylidene}amino)oxy]acetamide (**6l**).* Yield 88 %; m.p.182 °C; IR (υ, cm^{-1}): 3345 (N—H), 1598 (C=N), 1350 and 1161 (SO_2), 1559 (C=C); ^{1}H NMR (300 MHz, DMSO-d_6, ppm): 7.82–8.04 (4H, d, -Ar-H), 7.60 (2H, s-NH_2), 7.33–7.41 (5H, m, —Ar —H), 5.18 (2H, s, -CH_2), 3.39 (3H, s, -CH_3), 2.41 (3H, s, -CH_3); ^{13}C NMR (75 MHz, DMSO-d_6, ppm): 150.9, 145.6, 141.1, 138.6, 138.5, 133.2, 129.0 (2C), 128.8 (2C), 128.5, 127.8 (2C), 126.5 (2C), 76.1, 13.4, 11.1; $C_{18}H_{19}N_5O_3SH^+$: (ES-API, pos. ion): (M + 1) *m/z* = 386.1281, calcd. For 386.1287

*4.1.4.13. 4-(5-Methyl-4-{1-[(naphthalen-1-ylmethoxy)imino]ethyl}-1H-1,2,3-triazol-1-yl)benzenesulfonamide (**6m**).* Yield 91 %; m.p.163 °C; IR (υ, cm^{-1}): 3256 (N—H), 1628 (C=N), 1595 (C=C), 1355 and 1167 (SO2); ^{1}H NMR (300 MHz, DMSO-d_6, ppm): 8.02–8.18 (4H, d, -Ar-H), 7.61 (2H, s-NH_2), 7.49–7.96 (7H, m, —Ar —H), 5.65 (2H, s, -CH_2), 3.41 (3H, s, -CH_3), 2.40 (3H, s, -CH_3); ^{13}C NMR (75 MHz, DMSO-d_6, ppm): 150.9, 145.6, 141.1, 138.5, 134.0, 133.2, 131.9, 129.3, 129.1 (2C), 127.9, 127.8, 127.1, 126.6 (2C), 126.5, 126.0, 124.6 (2C), 74.7, 13.3, 11.2; $C_{22}H_{21}N_5O_3SH^+$: (ES-API, pos. ion): (M + 1) m/z = 436.1438, calcd. For 436.1443

*4.1.4.14. 4-(4-{1-[(Anthracen-9-ylmethoxy)imino]ethyl}-5-methyl-1H-1,2,3-triazol-1-yl)benzenesulfonamide (**6n**).* Yield 85 %; m.p.248 °C; IR (υ, cm^{-1}): 3259 (N—H), 1634 (C=N) 1594 (C=C), 1358 and 1168 (SO2); ^{1}HNMR (300 MHz, DMSO-d_6, ppm): 7.94–8.46 (4H, d, -Ar-H), 7.40–8.02 (9H, m, —Ar —H), 7.59 (2H, s-NH_2), 6.14 (2H, s, -CH_2), 2.49 (3H, s, -CH_3), 2.22 (3H, s, -CH_3); ^{13}C NMR (75 MHz, DMSO-d_6, ppm):150.8, 145.5, 141.2, 138.4, 132.6, 131.5, 131.2, 129.3 (2C), 128.9 (2C), 128.8 (3C), 127.8 (2C), 126.7, 125.8 (2C), 125.5 (2C), 124.9 (2C), 68.3, 12.9, 11.1; $C_{26}H_{23}N_5O_3SH^+$: (ES-API, pos. ion): (M + 1) m/z = 486.1595, calcd. For 485.1600

4.2. Carbonic anhydrase inhibitory effect study

In order to ascertain the inhibitory effects of novel 1,2,3-triazole benzenesulfonamide substituted oxime ether derivatives (**6a-n**), the esterase activity of the *h*CAs, *h*CA I, II, IX, and XII isoforms were examined using Verpoorte's method [59] of determining the change in absorbance at 348 nm [60–62]. At a starting concentration of 1 mg/mL, these oxime ethers (**6a-n**) and AAZ were dissolved in DMSO. In the final reaction mixture, DMSO was present at a concentration of around 1 %. As in other studies, the *h*CA isoforms' activity was evaluated using the substrate 4-nitrophenyl acetate (PubChem CID: 13243) [63–65]. An enzyme unit was defined as the quantity of enzyme needed to catalyze the reaction of 1 μmol of substrate per minute at 25 °C. Each sample underwent three measurements. In order to explore the in vitro inhibitory mechanisms of the 1,2,3-triazole linked benzenesulfonamides **6a-n**, we conducted kinetic assays with varying substrate and chemical concentrations. The obtained data were then employed to generate Michaelis-Menten curves [66] and Lineweaver-Burk plots [67], as well as to compute K_I values and identify the types of inhibition [68].

4.3. Cytotoxic activity study

Human breast adenocarcinoma (MCF-7), human liver adenocarcinoma (Hep—3B), and normal mouse fibroblast (L929) cell lines were obtained from the American Type Culture Collection (ATCC). The cells were cultured in DMEM medium supplemented with 2 mL L-glutamine, 10 % heat-inactivated fetal bovine serum, and 1 % penicillin/streptomycin according to routine culture protocols. All cells were maintained at 37 °C in a humidified atmosphere with 5 % CO_2. After culturing for 24 h, cell viability was determined using an MTT assay, as previously reported [69,70]. Optical density was measured at 570 nm using the ELISA plate reader. All the measurements were repeated thrice. $S_I^{(cell\ line)}$, the ratio of IC_{50} values calculated for healthy and cancer cells, was then determined as in previous studies [71,72].

4.4. In silico study

The most recent version, Small-Molecule Drug Discovery Suite 2022–3 for Mac, was employed for the molecular docking analysis (Schrödinger, LLC, NY, USA). For the *h*CA isoforms used as the model for the experiment, the PDB IDs 1AZM (*h*CA I, A chain, 2.00 Å) [52], 3HS4 (*h*CA II, A chain, 1.10 Å) [53], 3IAI (*h*CA IX, B chain, 2.20 Å) [54], and 1JD0 (*h*CA XII, A chain, 1.50 Å) [55] were retrieved from the RCSB Protein Data Bank (https://www.rcsb.org) [73]. In order to get the enzyme structures ready for docking, the suite's Protein Preparation Wizard was used [74,75]. ChemDraw program V21 for Mac was used to sketch the structures of the novel 1,2,3-triazole benzenesulfonamide substituted oxime ether derivatives (**6a-n**) (PerkinElmer, Inc., Waltham, MA, USA). The LigPrep module of the same software program [76–78] was used to optimize these oxime ethers (**6a-n**) at pH 7.4 ± 0.5 in the optimal potential liquid simulations 4 (OPLS4) force field with Epik [79–81]. To generate the receptor grid in the Maestro panel, the active site residues discovered by the SiteMap tool [82,83] were defined in the Receptor Grid Generation module [84]. With the default settings, the extra precision (XP) method of the Glide application [85–88] was employed to dock ligands to *h*CAs. Additionally, using the *h*CA-ligand complexes 1AZM, 3HS4, 3IAI, and 1JD0, it has been determined how effectively the MM-GBSA predicts [89] relative binding affinity in the VSGB energy model and OPLS force field [90,91].

4.5. Statistical study

The data was analyzed and graphical representation was produced using GraphPad Prism V9 for Mac (GraphPad Software, La Jolla California USA). K_I constants were calculated with SigmaPlot V12 for Windows (Systat Software, San Jose California USA). To compare the fit of enzyme inhibition models, the extra sum-of-squares *F* test and the AIC approach were used. Results were presented as mean ± standard error of the mean (95 % confidence intervals) and statistical significance was determined using a p-value <0.05.

Abbreviations

AAZ	acetazolamide
AIC	Akaike information criterion
ATCC	American type culture collection
DMF	dimethylformamide
DMSO	dimethylsulfoxide
*h*CA	human α-carbonic anhydrase
*h*CAIs	human α-carbonic anhydrase inhibitors
K_I	enzyme inhibition constants
R^2	K_I coefficient of determination
MM-GBSA	Molecular mechanics with generalized Born and surface area solvation
OPLS	optimal potential liquid simulations
SARs	structure-activity relationships
S_I	selectivity index
TBAB	tetrabutylammonium bromide

CRediT authorship contribution statement

Aida Buza: Formal analysis, Validation, and Investigation. Cüneyt Türkeş: Conceptualization, Methodology, Formal analysis, Validation, Investigation, Writing, and Funding acquisition. Mustafa Arslan: Conceptualization, Methodology, Formal analysis, Validation, Investigation, Writing, and Funding acquisition. Yeliz Demir: Formal analysis, Validation, and Investigation. Busra Dincer: Formal analysis, Validation, Investigation, and Writing. Arleta Rifati Nixha: Conceptualization and Methodology. Şükrü Beydemir: Conceptualization, Methodology, and Funding acquisition.

Declaration of competing interest

The authors declare that they have no known competing financial interests or personal relationships that could have appeared to influence the work reported in this paper.

Data availability

The data that support the findings of this study are available from the corresponding author upon reasonable request.

Acknowledgement

This work was supported by the Research Fund of Sakarya University (grant number 2020-9-32-85), the Research Fund of Erzincan Binali Yıldırım University (grant number TSA-2020-729), and the Research Fund of Anadolu University (grant number 2102S003).

Appendix A. Supplementary data

Supplementary data to this article can be found online at https://doi.org/10.1016/j.ijbiomac.2023.124232.

References

[1] N. Lolak, S. Akocak, M. Durgun, H.E. Duran, A. Necip, C. Türkeş, M. Işık, Ş. Beydemir, Novel bis-ureido-substituted sulfaguanidines and sulfisoxazoles as carbonic anhydrase and acetylcholinesterase inhibitors, Mol. Divers. (2022), https://doi.org/10.1007/s11030-022-10527-0.
[2] Y. Deng, B. Li, T. Zhang, Bacteria that make a meal of sulfonamide antibiotics: blind spots and emerging opportunities, Environ. Sci. Technol. 52 (7) (2018) 3854–3868, https://doi.org/10.1021/acs.est.7b06026.
[3] S.S. Stokes, R. Albert, E.T. Buurman, B. Andrews, A.B. Shapiro, O.M. Green, A. R. McKenzie, L.R. Otterbein, Inhibitors of the acetyltransferase domain of N-acetylglucosamine-1-phosphate-uridylyltransferase/glucosamine-1-phosphate-acetyltransferase (GlmU). Part 2: optimization of physical properties leading to antibacterial aryl sulfonamides, Bioorg. Med. Chem. Lett. 22 (23) (2012) 7019–7023, https://doi.org/10.1016/j.bmcl.2012.10.003.
[4] A.P. Keche, G.D. Hatnapure, R.H. Tale, A.H. Rodge, S.S. Birajdar, V.M. Kamble, A novel pyrimidine derivatives with aryl urea, thiourea and sulfonamide moieties: synthesis, anti-inflammatory and antimicrobial evaluation, Bioorg. Med. Chem. Lett. 22 (10) (2012) 3445–3448, https://doi.org/10.1016/j.bmcl.2012.03.092.
[5] L.F.C. da Costa Leite, R.H. Veras Mourão, M.d.C.A. de Lima, S.L. Galdino, M. Z. Hernandes, F. de Assis Rocha, S. Neves, J. Vidal, I. da Barbe, Rocha Pitta, Synthesis, biological evaluation and molecular modeling studies of arylidene-thiazolidinediones with potential hypoglycemic and hypolipidemic activities, Eur. J. Med. Chem. 42 (10) (2007) 1263–1271, https://doi.org/10.1016/j.ejmech.2007.02.015.
[6] R. Sharma, S.S. Soman, Design and synthesis of sulfonamide derivatives of pyrrolidine and piperidine as anti-diabetic agents, Eur. J. Med. Chem. 90 (2015) 342–350, https://doi.org/10.1016/j.ejmech.2014.11.041.
[7] E. Bilen, Ü. Özdemir Özmen, S. Çete, S. Alyar, A. Yaşar, Bioactive sulfonyl hydrazones with alkyl derivative: Characterization, ADME properties, molecular docking studies and investigation of inhibition on choline esterase enzymes for the diagnosis of Alzheimer's disease, Chem.-Biol. Interact. 360 (2022), 109956, https://doi.org/10.1016/j.cbi.2022.109956.
[8] D. Dheer, V. Singh, R. Shankar, Medicinal attributes of 1,2,3-triazoles: current developments, Bioorg. Chem. 71 (2017) 30–54, https://doi.org/10.1016/j.bioorg.2017.01.010.

[9] J.F. Remenar, S.L. Morissette, M.L. Peterson, B. Moulton, J.M. MacPhee, H. R. Guzmán, Ö. Almarsson, Crystal engineering of novel cocrystals of a triazole drug with 1,4-dicarboxylic acids, J. Am. Chem. Soc. 125 (28) (2003) 8456–8457, https://doi.org/10.1021/ja035776p.
[10] K. Kushwaha, N. Kaushik, S.C.Jain Lata, Design and synthesis of novel 2H-chromen-2-one derivatives bearing 1,2,3-triazole moiety as lead antimicrobials, Bioorg. Med. Chem. Lett. 24 (7) (2014) 1795–1801, https://doi.org/10.1016/j.bmcl.2014.02.027.
[11] F.Valério Lopes, P.H.Fazza Stroppa, J.A. Marinho, R.Reis Soares, L. de Azevedo Alves, P.V.Z.Capriles Goliatt, C. Abramo, A.David da Silva, 1,2,3-Triazole derivatives: synthesis, docking, cytotoxicity analysis and in vivo antimalarial activity, Chem.-Biol. Interact. 350 (2021), 109688, https://doi.org/10.1016/j.cbi.2021.109688.
[12] C. Zhou, Y. Wang, Recent researches in triazole compounds as medicinal drugs, Curr. Med. Chem. 19 (2) (2012) 239–280, https://doi.org/10.2174/092986712803414213.
[13] C. Lass-Flörl, Triazole antifungal agents in invasive fungal infections, Drugs 71 (18) (2011) 2405–2419, https://doi.org/10.2165/11596540-000000000-00000.
[14] H. Mughal, M. Szostak, Recent advances in the synthesis and reactivity of azetidines: strain-driven character of the four-membered heterocycle, Org. Biomol. Chem. 19 (15) (2021) 3274–3286, https://doi.org/10.1039/D1OB00061F.
[15] A. Rossello, S. Bertini, A. Lapucci, M. Macchia, A. Martinelli, S. Rapposelli, E. Herreros, B. Macchia, Synthesis, antifungal activity, and molecular modeling studies of new inverted oxime ethers of oxiconazole, J. Med. Chem. 45 (22) (2002) 4903–4912, https://doi.org/10.1021/jm020980t.
[16] M.N. Soltani Rad, S. Behrouz, E. Zarenezhad, M.H. Moslemin, A. Zarenezhad, M. Mardkhoshnood, M. Behrouz, S. Rostami, Synthesis of fluorene and/or benzophenone O-oxime ethers containing amino acid residues and study of their cardiovascular and antibacterial effects, Med. Chem. Res. 23 (8) (2014) 3810–3822, https://doi.org/10.1007/s00044-014-0967-3.
[17] M.I. El-Gamal, S.M. Bayomi, S.M. El-Ashry, S.A. Said, A.A.M. Abdel-Aziz, N. I. Abdel-Aziz, Synthesis and anti-inflammatory activity of novel (substituted) benzylidene acetone oxime ether derivatives: molecular modeling study, Eur. J. Med. Chem. 45 (4) (2010) 1403–1414, https://doi.org/10.1016/j.ejmech.2009.12.041.
[18] Z. Özdemir, S. Sari, A. Karakurt, S. Dalkara, Synthesis, anticonvulsant screening, and molecular modeling studies of new arylalkylimidazole oxime ether derivatives, Drug Dev. Res. 80 (2) (2019) 269–280, https://doi.org/10.1002/ddr.21491.
[19] M. Vágvölgyi, A. Martins, Á. Kulmány, I. Zupkó, T. Gáti, A. Simon, G. Tóth, A. Hunyadi, Nitrogen-containing ecdysteroid derivatives vs. multi-drug resistance in cancer: preparation and antitumor activity of oximes, oxime ethers and a lactam, Eur. J. Med. Chem. 144 (2018) 730–739, https://doi.org/10.1016/j.ejmech.2017.12.032.
[20] B. Sever, C. Türkeş, M.D. Altıntop, Y. Demir, Ş. Beydemir, Thiazolyl-pyrazoline derivatives: in vitro and in silico evaluation as potential acetylcholinesterase and carbonic anhydrase inhibitors, Int. J. Biol. Macromol. 163 (2020) 1970–1988, https://doi.org/10.1016/j.ijbiomac.2020.09.043.
[21] P. Taslimi, İ. Gülçin, N. Öztaşkın, Y. Çetinkaya, S. Göksu, S.H. Alwasel, C. T. Supuran, The effects of some bromophenols on human carbonic anhydrase isoenzymes, J. Enzyme Inhib. Med. Chem. 31 (4) (2016) 603–607, https://doi.org/10.3109/14756366.2015.1054820.
[22] Y. Thakur, M. Tripathi, B. Verma, R. Khilari, R. Agrawal, M. Khursheed Likheshwari, R. Siddiqi, E. Pande, R.H.Khan Mohapatra, Interaction of cobalt(II) and copper(II) hydroxamates with polyriboadenylic acid: an insight into RNA based drug designing, nucleosides, Nucleotides Nucleic Acids 38 (7) (2019) 481–508, https://doi.org/10.1080/15257770.2018.1562074.
[23] K. Pedrood, M. Sherafati, M. Mohammadi-Khanaposhtani, M.S. Asgari, S. Hosseini, H. Rastegar, B. Larijani, M. Mahdavi, P. Taslimi, Y. Erden, S. Günay, İ. Gulçin, Design, synthesis, characterization, enzymatic inhibition evaluations, and docking study of novel quinazolinone derivatives, Int. J. Biol. Macromol. 170 (2021) 1–12, https://doi.org/10.1016/j.ijbiomac.2020.12.121.
[24] A.H. Eldeeb, M.F. Abo-Ashour, A. Angeli, A. Bonardi, D.S. Lasheen, E.Z. Elrazaz, A. Nocentini, P. Gratteri, H.A. Abdel-Aziz, C.T. Supuran, Novel benzenesulfonamides aryl and arylsulfone conjugates adopting tail/dual tail approaches: synthesis, carbonic anhydrase inhibitory activity and molecular modeling studies, Eur. J. Med. Chem. 221 (2021), 113486, https://doi.org/10.1016/j.ejmech.2021.113486.
[25] F. Topal, I. Gulcin, A. Dastan, M. Guney, Novel eugenol derivatives: potent acetylcholinesterase and carbonic anhydrase inhibitors, Int. J. Biol. Macromol. 94 (2017) 845–851, https://doi.org/10.1016/j.ijbiomac.2016.10.096.
[26] S. Manzoor, A. Petreni, M.K. Raza, C.T. Supuran, N. Hoda, Novel triazole-sulfonamide bearing pyrimidine moieties with carbonic anhydrase inhibitory action: design, synthesis, computational and enzyme inhibition studies, Bioorg. Med. Chem. Lett. 48 (2021), 128249, https://doi.org/10.1016/j.bmcl.2021.128249.
[27] A. Cecchi, A. Hulikova, J. Pastorek, S. Pastoreková, A. Scozzafava, J.-Y. Winum, J.-L. Montero, C.T. Supuran, Carbonic anhydrase inhibitors. Design of fluorescent sulfonamides as probes of tumor-associated carbonic anhydrase IX that inhibit isozyme IX-mediated acidification of hypoxic tumors, J. Med. Chem. 48 (15) (2005) 4834–4841, https://doi.org/10.1021/jm0501073.
[28] Y. Demir, C. Türkeş, M.S. Çavuş, M. Erdoğan, H. Muğlu, H. Yakan, Ş. Beydemir, Enzyme inhibition, molecular docking, and density functional theory studies of new thiosemicarbazones incorporating the 4-hydroxy-3,5-dimethoxy benzaldehyde motif, Arch. Pharm. 356 (2023), e2200554, https://doi.org/10.1002/ardp.202200554. Weinheim, Ger.
[29] C.T. Supuran, Carbon- versus Sulphur-based zinc binding groups for carbonic anhydrase inhibitors? J. Enzyme Inhib. Med. Chem. 33 (1) (2018) 485–495, https://doi.org/10.1080/14756366.2018.1428572.
[30] A.J. Esbaugh, B.L. Tufts, The structure and function of carbonic anhydrase isozymes in the respiratory system of vertebrates, Resp. Phys. Neurobiol. 154 (1) (2006) 185–198, https://doi.org/10.1016/j.resp.2006.03.007.
[31] V. Alterio, A.Di Fiore, K. D'Ambrosio, C.T. Supuran, G.De Simone, Multiple binding modes of inhibitors to carbonic anhydrases: how to design specific drugs targeting 15 different isoforms? Chem. Rev. 112 (8) (2012) 4421–4468, https://doi.org/10.1021/cr200176r. Washington, DC, U. S.
[32] R. Kumar, L. Vats, S. Bua, C.T. Supuran, P.K. Sharma, Design and synthesis of novel benzenesulfonamide containing 1,2,3-triazoles as potent human carbonic anhydrase isoforms I, II, IV and IX inhibitors, Eur. J. Med. Chem. 155 (2018) 545–551, https://doi.org/10.1016/j.ejmech.2018.06.021.
[33] S.A. Güngör, M. Köse, M. Tümer, C. Türkeş, Ş. Beydemir, Synthesis, characterization and docking studies of benzenesulfonamide derivatives containing 1,2,3-triazole as potential ınhibitor of carbonic anhydrase I-II enzymes, J. Biomol. Struct. Dyn. (2022) 1–11, https://doi.org/10.1080/07391102.2022.2159531.
[34] C.T. Supuran, Carbonic anhydrase inhibitors, Bioorg. Med. Chem. Lett. 20 (12) (2010) 3467–3474, https://doi.org/10.1016/j.bmcl.2010.05.009.
[35] A. Scozzafava, M. Passaponti, C.T. Supuran, İ. Gülçin, Carbonic anhydrase inhibitors: guaiacol and catechol derivatives effectively inhibit certain human carbonic anhydrase isoenzymes (hCA I, II, IX and XII), J. Enzyme Inhib. Med. Chem. 30 (4) (2015) 586–591, https://doi.org/10.3109/14756366.2014.956310.
[36] A. Scozzafava, P. Kalın, C.T. Supuran, İ. Gülçin, S.H. Alwasel, The impact of hydroquinone on acetylcholine esterase and certain human carbonic anhydrase isoenzymes (hCA I, II, IX, and XII), J. Enzyme Inhib. Med. Chem. 30 (6) (2015) 941–946, https://doi.org/10.3109/14756366.2014.999236.
[37] C.T. Supuran, A. Scozzafava, Carbonic anhydrases as targets for medicinal chemistry, Bioorg. Med. Chem. 15 (13) (2007) 4336–4350, https://doi.org/10.1016/j.bmc.2007.04.020.
[38] R.E. Bora, H.G. Bilgicli, E.M. Üç, M.A. Alagöz, M. Zengin, İ. Gulcin, Synthesis, characterization, evaluation of metabolic enzyme inhibitors and in silico studies of thymol based 2-amino thiol and sulfonic acid compounds, Chem. Biol. Interact. (2022), 110134, https://doi.org/10.1016/j.cbi.2022.110134.
[39] K. Yararli, E.B. Ozer, S. Bayindir, C. Caglayan, C. Turkes, S. Beydemir, The synthesis, biological evaluation and in silico studies of asymmetric 3,5-diaryl-rhodanines as novel inhibitors of human carbonic anhydrase isoenzymes, J. Mol. Struct. 1276 (2023), 134783, https://doi.org/10.1016/j.molstruc.2022.134783.
[40] V. Sharma, R. Kumar, A. Angeli, C.T. Supuran, P.K. Sharma, Tail approach synthesis of novel benzenesulfonamides incorporating 1,3,4-oxadiazole hybrids as potent inhibitor of carbonic anhydrase I, II, IX, and XII isoenzymes, Eur. J. Med. Chem. 193 (2020), 112219, https://doi.org/10.1016/j.ejmech.2020.112219.
[41] C.T. Supuran, How many carbonic anhydrase inhibition mechanisms exist? J. Enzyme Inhib. Med. Chem. 31 (3) (2016) 345–360, https://doi.org/10.3109/14756366.2015.1122001.
[42] J. Ivanova, J. Leitans, M. Tanc, A. Kazaks, R. Zalubovskis, C.T. Supuran, K. Tars, X-ray crystallography-promoted drug design of carbonic anhydrase inhibitors, Chem. Commun. 51 (33) (2015) 7108–7111, https://doi.org/10.1039/C5CC01854D. Cambridge, U. K.
[43] R.P. Tanpure, B. Ren, T.S. Peat, L.F. Bornaghi, D. Vullo, C.T. Supuran, S.-A. Poulsen, Carbonic anhydrase inhibitors with dual-tail moieties to match the hydrophobic and hydrophilic halves of the carbonic anhydrase active site, J. Med. Chem. 58 (3) (2015) 1494–1501, https://doi.org/10.1021/jm501798g.
[44] A. Bonardi, A. Nocentini, S. Bua, J. Combs, C. Lomelino, J. Andring, L. Lucarini, S. Sgambellone, E. Masini, R. McKenna, P. Gratteri, C.T. Supuran, Sulfonamide inhibitors of human carbonic anhydrases designed through a three-tails approach: improving ligand/isoform matching and selectivity of action, J. Med. Chem. 63 (13) (2020) 7422–7444, https://doi.org/10.1021/acs.jmedchem.0c00733.
[45] C.T. Supuran, Exploring the multiple binding modes of inhibitors to carbonic anhydrases for novel drug discovery, Expert Opin. Drug Discovery 15 (6) (2020) 671–686, https://doi.org/10.1080/17460441.2020.1743676.
[46] C. Kakakhan, C. Türkeş, Ö. Güleç, Y. Demir, M. Arslan, G. Özkemahlı, Ş. Beydemir, Exploration of 1,2,3-triazole linked benzenesulfonamide derivatives as isoform selective inhibitors of human carbonic anhydrase, Bioorg. Med. Chem. 77 (2023), 117111, https://doi.org/10.1016/j.bmc.2022.117111.
[47] M. Bozdag, M. Ferraroni, E. Nuti, D. Vullo, A. Rossello, F. Carta, A. Scozzafava, C. T. Supuran, Combining the tail and the ring approaches for obtaining potent and isoform-selective carbonic anhydrase inhibitors: solution and X-ray crystallographic studies, Bioorg. Med. Chem. 22 (1) (2014) 334–340, https://doi.org/10.1016/j.bmc.2013.11.016.
[48] A. Nocentini, C.T. Supuran, Advances in the structural annotation of human carbonic anhydrases and impact on future drug discovery, Expert Opin. Drug Discovery 14 (11) (2019) 1175–1197, https://doi.org/10.1080/17460441.2019.1651289.
[49] S. Kılıcaslan, M. Arslan, Z. Ruya, Ç. Bilen, A. Ergün, N. Gençer, O. Arslan, Synthesis and evaluation of sulfonamide-bearing thiazole as carbonic anhydrase isoforms hCA I and hCA II, J. Enzyme Inhib. Med. Chem. 31 (6) (2016) 1300–1305, https://doi.org/10.3109/14756366.2015.1128426.
[50] M.A. Pinard, B. Mahon, R. McKenna, Probing the surface of human carbonic anhydrase for clues towards the design of isoform specific inhibitors, Biomed. Res. Int. 2015 (2015), 453543, https://doi.org/10.1155/2015/453543.
[51] J.J. Lica, M. Wieczór, G.J. Grabe, M. Heldt, M. Jancz, M. Misiak, K. Gucwa, W. Brankiewicz, N. Maciejewska, A. Stupak, Effective drug concentration and selectivity depends on fraction of primitive cells, Int. J. Mol. Sci. 22 (9) (2021) 4931, https://doi.org/10.3390/ijms22094931.

[52] S. Chakravarty, K.K. Kannan, Drug-protein interactions: refined structures of three sulfonamide drug complexes of human carbonic anhydrase I enzyme, J. Mol. Biol. 243 (2) (1994) 298–309, https://doi.org/10.1006/jmbi.1994.1655.
[53] K.H. Sippel, A.H. Robbins, J. Domsic, C. Genis, M. Agbandje-McKenna, R. McKenna, High-resolution structure of human carbonic anhydrase II complexed with acetazolamide reveals insights into inhibitor drug design, Acta Crystallogr. Sect. F: Struct. Biol. Cryst. Commun. 65 (10) (2009) 992–995, https://doi.org/10.1107/S1744309109036665.
[54] V. Alterio, M. Hilvo, A. Di Fiore, C.T. Supuran, P. Pan, S. Parkkila, A. Scaloni, J. Pastorek, S. Pastorekova, C. Pedone, Crystal structure of the catalytic domain of the tumor-associated human carbonic anhydrase IX, Proc. Natl. Acad. Sci. India Sect. A 106 (38) (2009) 16233–16238, https://doi.org/10.1073/pnas.0908301106.
[55] D.A. Whittington, A. Waheed, B. Ulmasov, G.N. Shah, J.H. Grubb, W.S. Sly, D. W. Christianson, Crystal structure of the dimeric extracellular domain of human carbonic anhydrase XII, a bitopic membrane protein overexpressed in certain cancer tumor cells, Proc. Natl. Acad. Sci. India Sect. A 98 (17) (2001) 9545–9550, https://doi.org/10.1073/pnas.16130129.
[56] C.A. Lipinski, F. Lombardo, B.W. Dominy, P.J. Feeney, Experimental and computational approaches to estimate solubility and permeability in drug discovery and development settings, Adv. Drug Deliv. Rev. 23 (1) (1997) 3–25, https://doi.org/10.1016/S0169-409X(96)00423-1.
[57] E.M. Duffy, W.L. Jorgensen, Prediction of properties from simulations: free energies of solvation in hexadecane, octanol, and water, J. Am. Chem. Soc. 122 (12) (2000) 2878–2888, https://doi.org/10.1021/ja993663t.
[58] J.B. Baell, G.A. Holloway, New substructure filters for removal of pan assay interference compounds (PAINS) from screening libraries and for their exclusion in bioassays, J. Med. Chem. 53 (7) (2010) 2719–2740, https://doi.org/10.1021/jm901137j.
[59] J.A. Verpoorte, S. Mehta, J.T. Edsall, Esterase activities of human carbonic anhydrases B and C, J. Biol. Chem. 242 (18) (1967) 4221–4229, https://doi.org/10.1016/S0021-9258(18)95800-X.
[60] C. Türkeş, M. Arslan, Y. Demir, L. Cocaj, A.R. Nixha, Ş. Beydemir, Synthesis, biological evaluation and in silico studies of novel N-substituted phthalazine sulfonamide compounds as potent carbonic anhydrase and acetylcholinesterase inhibitors, Bioorg. Chem. 89 (2019), 103004, https://doi.org/10.1016/j.bioorg.2019.103004.
[61] C. Türkeş, Y. Demir, Ş. Beydemir, Calcium channel blockers: molecular docking and inhibition studies on carbonic anhydrase I and II isoenzymes, J. Biomol. Struct. Dyn. 39 (5) (2021) 1672–1680, https://doi.org/10.1080/07391102.2020.1736631.
[62] B. Sever, C. Türkeş, M.D. Altıntop, Y. Demir, G.A. Çiftçi, Ş. Beydemir, Novel metabolic enzyme inhibitors designed through the molecular hybridization of thiazole and pyrazoline scaffolds, Arch. Pharm. 354 (12) (2021), e2100294, https://doi.org/10.1002/ardp.202100294. Weinheim, Ger.
[63] D. Osmaniye, C. Türkeş, Y. Demir, Y. Özkay, Ş. Beydemir, Z.A. Kaplancıklı, Design, synthesis, and biological activity of novel dithiocarbamate-methylsulfonyl hybrides as carbonic anhydrase inhibitors, Arch. Pharm. 355 (2022), e2200132, https://doi.org/10.1002/ardp.202200132. Weinheim, Ger.
[64] N. Lolak, S. Akocak, C. Türkeş, P. Taslimi, M. Işık, Ş. Beydemir, İ. Gülçin, M. Durgun, Synthesis, characterization, inhibition effects, and molecular docking studies as acetylcholinesterase, α-glycosidase, and carbonic anhydrase inhibitors of novel benzenesulfonamides incorporating 1,3,5-triazine structural motifs, Bioorg. Chem. 100 (2020), 103897, https://doi.org/10.1016/j.bioorg.2020.103897.
[65] A. Kilic, L. Beyazsakal, M. Işık, C. Türkeş, A. Necip, K. Takım, Ş. Beydemir, Mannich reaction derived novel boron complexes with amine-bis(phenolate) ligands: synthesis, spectroscopy and in vitro/in silico biological studies, J. Organomet. Chem. 927 (2020), 121542, https://doi.org/10.1016/j.jorganchem.2020.121542.
[66] I.N. Korkmaz, C. Türkeş, Y. Demir, H. Özdemir, Ş. Beydemir, Methyl benzoate derivatives: in vitro paraoxonase 1 inhibition and in silico studies, J. Biochem. Mol. Toxicol. 36 (10) (2022), e23152, https://doi.org/10.1002/jbt.23152.
[67] H. Lineweaver, D. Burk, The determination of enzyme dissociation constants, J. Am. Chem. Soc. 56 (3) (1934) 658–666, https://doi.org/10.1021/ja01318a036.
[68] C. Türkeş, S. Akocak, M. Işık, N. Lolak, P. Taslimi, M. Durgun, İ. Gülçin, Y. Budak, Ş. Beydemir, Novel inhibitors with sulfamethazine backbone: synthesis and biological study of multi-target cholinesterases and α-glucosidase inhibitors, J. Biomol. Struct. Dyn. 40 (19) (2022) 8752–8764, https://doi.org/10.1080/07391102.2021.1916599.
[69] T. Mosmann, Rapid colorimetric assay for cellular growth and survival: application to proliferation and cytotoxicity assays, J. Immunol. Methods 65 (1) (1983) 55–63, https://doi.org/10.1016/0022-1759(83)90303-4.
[70] P. Kumar, A. Nagarajan, P.D. Uchil, Analysis of cell viability by the lactate dehydrogenase assay, Cold Spring Harb. Protoc. 2018 (6)) (2018), pdb.prot095497, https://doi.org/10.1101/pdb.prot095497.
[71] R.B. Badisa, S.F. Darling-Reed, P. Joseph, J.S. Cooperwood, L.M. Latinwo, C. B. Goodman, Selective cytotoxic activities of two novel synthetic drugs on human breast carcinoma MCF-7 cells, Anticancer Res. 29 (8) (2009) 2993–2996.
[72] J. Krzywik, W. Mozga, M. Aminpour, J. Janczak, E. Maj, J. Wietrzyk, J. A. Tuszyński, A. Huczyński, Synthesis, antiproliferative activity and molecular docking studies of novel doubly modified colchicine amides and sulfonamides as anticancer agents, Molecules 25 (8) (2020) 1789, https://doi.org/10.3390/molecules25081789.
[73] M. Durgun, C. Türkeş, M. Işık, Y. Demir, A. Saklı, A. Kuru, A. Güzel, Ş. Beydemir, S. Akocak, S.M. Osman, Z. AlOthman, C.T. Supuran, Synthesis, characterization, biological evaluation and in silico studies of sulfonamide schiff bases, J. Enzyme Inhib. Med. Chem. 35 (1) (2020) 950–962, https://doi.org/10.1080/14756366.2020.1746784.
[74] Schrödinger Release 2022-3: Protein Preparation Wizard, Schrödinger, LLC, New York, NY, 2022.
[75] G. Madhavi Sastry, M. Adzhigirey, T. Day, R. Annabhimoju, W. Sherman, Protein and ligand preparation: parameters, protocols, and influence on virtual screening enrichments, J. Comput. Aided Mol. Des. 27 (3) (2013) 221–234, https://doi.org/10.1007/s10822-013-9644-8.
[76] Schrödinger Release 2022-3: LigPrep, Schrödinger, LLC, New York, NY, 2022.
[77] S. Askin, H. Tahtaci, C. Türkeş, Y. Demir, A. Ece, G.A. Çiftçi, Ş. Beydemir, Design, synthesis, characterization, in vitro and in silico evaluation of novel imidazo [2, 1-b][1, 3, 4] thiadiazoles as highly potent acetylcholinesterase and non-classical carbonic anhydrase inhibitors, Bioorg. Chem. (2021), 105009, https://doi.org/10.1016/j.bioorg.2021.105009.
[78] Y. Demir, H. Ceylan, C. Türkeş, Ş. Beydemir, Molecular docking and inhibition studies of vulpinic, carnosic and usnic acids on polyol pathway enzymes, J. Biomol. Struct. Dyn. 40 (22) (2022) 12008–12021, https://doi.org/10.1080/07391102.2021.1967195.
[79] Schrödinger Release 2022-3: Epik, Schrödinger, LLC, New York, NY, 2022.
[80] J.C. Shelley, A. Cholleti, L.L. Frye, J.R. Greenwood, M.R. Timlin, M. Uchimaya, Epik: a software program for pKaprediction and protonation state generation for drug-like molecules, J. Comput. Aided Mol. Des. 21 (12) (2007) 681–691, https://doi.org/10.1007/s10822-007-9133-z.
[81] B. Sever, M.D. Altıntop, Y. Demir, C. Türkeş, K. Özbaş, G.A. Çiftçi, Ş. Beydemir, A. Özdemir, A new series of 2,4-thiazolidinediones endowed with potent aldose reductase inhibitory activity, Open Chem. 19 (2021) 347–357, https://doi.org/10.1515/chem-2021-0032.
[82] Schrödinger Release 2022-3: SiteMap, Schrödinger, LLC, New York, NY, 2022.
[83] T.A. Halgren, Identifying and characterizing binding sites and assessing druggability, J. Chem. Inf. Model. 49 (2) (2009) 377–389, https://doi.org/10.1021/ci800324m.
[84] Schrödinger Release 2022-3: Receptor Grid Generation, Schrödinger, LLC, New York, NY, 2022.
[85] Schrödinger Release 2022-3: Glide, Schrödinger, LLC, New York, NY, 2022.
[86] R.A. Friesner, J.L. Banks, R.B. Murphy, T.A. Halgren, J.J. Klicic, D.T. Mainz, M. P. Repasky, E.H. Knoll, M. Shelley, J.K. Perry, D.E. Shaw, P. Francis, P.S. Shenkin, Glide: a new approach for rapid, accurate docking and scoring. 1. Method and assessment of docking accuracy, J. Med. Chem. 47 (7) (2004) 1739–1749, https://doi.org/10.1021/jm0306430.
[87] T.A. Halgren, R.B. Murphy, R.A. Friesner, H.S. Beard, L.L. Frye, W.T. Pollard, J. L. Banks, Glide: a new approach for rapid, accurate docking and scoring. 2. Enrichment factors in database screening, J. Med. Chem. 47 (7) (2004) 1750–1759, https://doi.org/10.1021/jm030644s.
[88] Ö. Güleç, C. Türkeş, M. Arslan, Y. Demir, Y. Yeni, A. Hacımüftüoğlu, E. Ereminsoy, Ö.İ. Küfrevioğlu, Ş. Beydemir, Cytotoxic effect, enzyme inhibition, and in silico studies of some novel N-substituted sulfonyl amides incorporating 1,3,4-oxadiazol structural motif, Mol. Divers. 26 (2022) 2825–2845, https://doi.org/10.1007/s11030-022-10422-8.
[89] G. Barreiro, C.R.W. Guimarães, I. Tubert-Brohman, T.M. Lyons, J. Tirado-Rives, W. L. Jorgensen, Search for non-nucleoside inhibitors of HIV-1 reverse transcriptase using chemical similarity, molecular docking, and MM-GB/SA scoring, J. Chem. Inf. Model. 47 (6) (2007) 2416–2428, https://doi.org/10.1021/ci700271z.
[90] Schrödinger Release 2022-3: Prime, Schrödinger, LLC, New York, NY, 2022.
[91] G. Yapar, H.E. Duran, N. Lolak, S. Akocak, C. Türkeş, M. Durgun, M. Işık, Ş. Beydemir, Biological effects of bis-hydrazone compounds bearing isovanillin moiety on the aldose reductase, Bioorg. Chem. 117 (2021), 105473, https://doi.org/10.1016/j.bioorg.2021.105473.